Annu. Rev. Fluid Mech. 1993. 25 : 55–97

RESONANT INTERACTIONS AMONG SURFACE WATER WAVES

J. L. Hammack

Departments of Geosciences and Mathematics, The Pennsylvania State University, University Park, Pennsylvania 16802

D. M. Henderson

Department of Mathematics, The Pennsylvania State University, University Park, Pennsylvania 16802

KEY WORDS: nonlinear dynamics, gravity-capillary waves, dispersive waves

INTRODUCTION

Thirty years have passed since Phillips (1960) pioneered a view of weak, nonlinear interactions among gravity waves on the surface of deep water. His view emphasized the special role of "resonant" interactions, so-called because they have the mathematical form of a resonantly forced, linear oscillator. Unlike weak nonresonant interactions, weak resonant interactions can cause significant energy transfer among wavetrains and profoundly affect wavefield evolution. Early skepticism[1] of Phillips' view was dispelled unequivocally by experiments presented in the companion papers of Longuet-Higgins & Smith (1966) and McGoldrick et al (1966). This experimental confirmation of RIT (resonant interaction theory) and RIT's general applicability to a variety of phenomena (Benney 1962) made it one of the principle catalysts for the rapid expansion in the understanding of nonlinear wave phenomena that has occurred during the last thirty years.

[1] See the discussion comments in Section 4, pages 163–200, of *Ocean Wave Spectra Proceedings of a Conference* (1963) held in Easton, Maryland, May 1–4, 1961.

0066-4189/93/0115-0055$02.00

Ten years have passed since Phillips (1981a) presented a retrospective of resonant interaction theory which noted its maturity and suggested that it might be approaching its limits of usefulness. The maturity of RIT then and its older age now are evidenced by the plethora of literature which include review articles (Phillips 1967, 1974, 1981a; Yuen & Lake 1980, 1982) and comprehensive descriptions in monographs (Phillips 1977, LeBlond & Mysak 1978, West 1981, Ablowitz & Segur 1981, Craik 1985). Because of this maturity and the preponderance of readily available survey material this review is narrowly focused. In particular, we do not review coupling between surface and internal waves, internal waves, planetary waves, trapped waves, or waves in shallow water. Our objective is to review resonant interaction theories and experiments for waves on the surface of a deep layer of water. RIT is more than a framework for unifying wave phenomena—RIT is predictive. In fact, it provides one of the few analytically tractable models (the three-wave equations) of weak interactions among wavetrains with arbitrary wavelengths and directions of propagation. Yet, quantitative comparisons between RIT and RIE (resonant interaction experiments) are rarer than generally believed. Moreover, the success of RIT in quantitatively predicting the outcome of experiments is less established than generally believed. The theme of this review is that although RIT is mature, RIE is not, and perhaps its maturing will provide the basis for further theoretical developments.

An outline of the review is as follows. First, we review RIT in a variety of dynamical settings with an emphasis on the underlying approximations. We examine the elementary interactions of three- and four-wave resonances as well as deterministic and stochastic models for wavefields comprising either a broad or narrow spectrum of waves interacting in multiple and coupled sets. We also review some special settings in which higher-order resonances have been examined. Second, we review RIE in a variety of dynamical settings with an emphasis on those aspects that are predicted. We begin with a review of experimental investigations on the applicability of Kelvin's dispersion relation. We then review experiments involving gravity, gravity-capillary, and capillary wavetrains. We conclude by briefly summarizing results from comparisons between RIT and RIE and by noting the particularly glaring absence of controlled experiments in some applications.

RESONANT INTERACTION THEORY

In order to emphasize the basic notions of RIT and the generality of its application, we briefly outline its development for an arbitrary, nonlinear, energy conserving dynamical system. This outline, which closely parallels

Segur (1984) and Craik (1985), leads to necessary kinematical conditions for the existence of resonance, which underlie all applications of RIT. We then review a variety of dynamical analyses for surface waves in deep water that lie within the framework of RIT.

Basic Notions and Kinematical Considerations

Consider a nonlinear, energy-conserving dynamical system represented by

$$N(\phi) = 0, \tag{1}$$

in which N is a nonlinear operator, $\phi(\mathbf{x}, t)$ is a solution of (1), $\mathbf{x} = (x, y, z)$ is a position vector, and t is time. Suppose $\phi = 0$ is a (neutrally) stable equilibrium solution of (1), e.g. the quiescent surface for water waves. Infinitesimal deformations from this equilibrium state are found by linearizing (1) to obtain

$$L(\phi_1) = 0, \tag{2}$$

in which L is a linear operator and ϕ_1 is a solution of (2). If L has constant coefficients as it does for water waves, ϕ_1 has the form:

$$\phi_1 \sim \exp[i(\mathbf{k} \cdot \mathbf{x} - \omega t)], \tag{3}$$

in which $\mathbf{k} = (k_i) = (l, m, n)$ is a wavenumber vector (or simply wavevector) and ω is the wave frequency. Substituting (3) into (2) yields a dispersion relation for the linear problem:

$$\omega = W(\mathbf{k}). \tag{4a}$$

We require that ω exists in the sense that for fixed $\mathbf{k}$ there is a countable set of possible values for ω and that $W(\mathbf{k})$ is real-valued for real-valued $\mathbf{k}$. We also require that waves are nontrivially dispersive (Whitham 1974, p. 365), i.e.

$$\det\left(\frac{\partial^2 W(\mathbf{k})}{\partial k_i \partial k_j}\right) \neq 0, \qquad (i, j = 1, 2, 3). \tag{4b}$$

(Hence, in the context of water waves we avoid shallow water.) Now return to (1) and seek small-but-finite deformations from the equilibrium state by means of a formal power series:

$$\phi(\mathbf{x}, t; \varepsilon) = \sum_{r=1}^{\infty} \varepsilon^r \phi_r(\mathbf{x}, t), \qquad 0 < \varepsilon \ll 1. \tag{5}$$

At $O(\varepsilon)$ of (5), ϕ_1 satisfies (2) and can be represented by a superposition of S linear wavetrains, i.e.

$$\phi_1 = \sum_{s=1}^{S} (A_s e^{i\theta_s} + A_s^* e^{-i\theta_s}), \tag{6a}$$

in which A_s is the complex amplitude, A_s^* is its complex conjugate, and

$$\theta_s = \mathbf{k}_s \cdot \mathbf{x} - \omega_s t, \tag{6b}$$

is the wave phase. At this order, the S wavetrains interact linearly. The first nonlinear interactions appear at $O(\varepsilon^2)$ for which

$$L(\phi_2) = Q(\phi_1), \tag{7}$$

where Q is a quadratic operator. For definiteness, suppose we examine the nonlinear interactions between two wavetrains ($S = 2$); then Q yields terms like:

$$Q(\phi_1) = A_1 A_1^* + A_1^2 e^{i2\theta_1} + A_1^{*2} e^{-i2\theta_1} + A_1 A_2 e^{i(\theta_1+\theta_2)} + A_1 A_2^* e^{i(\theta_1-\theta_2)} + \cdots \tag{8}$$

The first three terms in (8) represent self-interactions of wavetrain $s = 1$; the first term corresponds to its mean flow while the second and third terms correspond to its second harmonic. The other terms shown in (8), and their complex conjugates, correspond to sum and difference wavetrains formed by nonlinear interactions between wavetrains $s = 1$ and $s = 2$. Supposing these quadratic interactions do not vanish identically we can examine the terms of (8) to see if any satisfy the dispersion relation of (4), i.e. we define

$$\theta_1 \pm \theta_2 = \theta_3 \quad \text{or} \quad (\mathbf{k}_1 \pm \mathbf{k}_2) \cdot \mathbf{x} - (\omega_1 \pm \omega_2) t = \pm \mathbf{k}_3 \cdot \mathbf{x} - (\pm \omega_3) t. \tag{9}$$

[The second-harmonic terms in (8) are a special case of (9) with $\theta_1 = \theta_2$.] If $(\mathbf{k}_3, \omega_3)$ satisfy (4), then (7) is the equation of a resonantly forced, linear oscillator. Hence, ϕ_2 will grow linearly in time so that the underlying assumption of small deformations in (5) is violated when $\varepsilon t = O(1)$. When the dispersion relation satisfies $W(\mathbf{k}) = -W(-\mathbf{k})$, as in water waves, we can write (9) in the form

$$\mathbf{k}_1 = \mathbf{k}_2 \pm \mathbf{k}_3, \tag{10a}$$

$$\omega_1 = \omega_2 \pm \omega_3. \tag{10b}$$

Equations (10) are necessary conditions for resonant three-wave interactions. The special case of $\theta_1 = \theta_2$ in (9) is termed second-harmonic (or internal) resonance. Phillips (1960) showed that resonant triads are not possible for deep-water gravity waves. McGoldrick (1965) showed that both second-harmonic and triadic resonances are possible for deep-water gravity-capillary waves. Second-harmonic resonance was originally noted by Harrison (1909) and investigated by Wilton (1915). Known as Wilton

ripples, second-harmonic resonance occurs for a wavetrain with wavenumber $k_0 = (\varrho g/2T)^{1/2}$, in which ϱ is the mass density, T is the surface tension, and g is the gravitational force per unit mass. [Triadic resonances also occur in shallow water where waves are nondispersive at leading order so that (10) are satisfied somewhat trivially.]

Proceeding to $O(\varepsilon^3)$, in which cubic nonlinear interactions occur on the right-hand side of (7), we allow three wavetrains ($S = 3$) in (6a). Then, assuming that triadic resonances do not occur, considerations similar to those above lead to necessary conditions for four-wave resonances:

$$\mathbf{k}_1 + \mathbf{k}_2 = \mathbf{k}_3 + \mathbf{k}_4, \tag{11a}$$

$$\omega_1 + \omega_2 = \omega_3 + \omega_4, \tag{11b}$$

in which we have made use of a dynamical result of Hasselmann (1962) to eliminate the usual $\pm$ signs. If Equations (11) are satisfied, the underlying assumption of small deformations in (5) is violated when $\varepsilon^2 t = O(1)$. Equations (11) include the special case of third-harmonic (internal) resonance as well as the degenerate case with $\omega_1 = \omega_2 = \omega_3 = \omega_4$ and $|\mathbf{k}_1| = |\mathbf{k}_2| = |\mathbf{k}_3| = |\mathbf{k}_4|$, i.e. the wavevectors in (11a) form a rhombus. Since a single wavetrain satisfies the latter degenerate case with collinear wavevectors, quartic resonances—unlike triadic resonances—are possible for any system. Phillips (1960) first showed that nondegenerate quartic resonances are the first to occur for gravity waves on deep water.

The above procedure can be continued for resonant quintets, sextets, etc; however, RIT in this general form is typically not exploited beyond triadic and quartic resonances. The reasons are twofold. Philosophically, it is generally assumed that the lowest-order resonant interactions that occur will dominate wavefield evolution; hence, the inevitable existence of resonant quartets mitigates interest in higher-order effects. In practice, the labor involved in the dynamical calculations of higher-order resonances is daunting. Nevertheless, the perturbative approach of RIT has been extended to higher-order resonances in some special cases which we discuss subsequently.

Dynamical Considerations

When the kinematical conditions of (10) or (11) are satisfied, a separate dynamical analysis is required to follow long-time evolution of the wavefield. Dynamical analyses have branched in several directions depending on the number of resonant wave sets possible for the underlying (linear) wavefield of (6a).

ELEMENTARY INTERACTIONS In the simplest cases, which we term elementary resonant interactions, a single triad or a single quartet of waves is

studied. Two common methods of analysis are the method of multiple scales (e.g. Benney 1962, McGoldrick 1965) and variational techniques (e.g. Simmons 1969). Both methods lead to a set of coupled, nonlinear partial differential equations for the complex amplitudes of the interacting wavetrains. These equations are similar for all dynamical systems, differing only in real-valued interaction coefficients, which depend on the linear properties of the underlying wavetrains. The equations for a single resonant triad (Ball 1964, Bretherton 1964, McGoldrick 1965, Benney & Newell 1967, Simmons 1969) can be written in the general form

$$(\partial_t + \mathbf{U}_s \cdot \nabla) A_s = i\gamma_s A^*_{s+1} A^*_{s+2}, \tag{12}$$

in which s is interpreted modulo 3, γ_s are the interaction coefficients, and $\mathbf{U}_s = \partial W(\mathbf{k}_s)/\partial \mathbf{k}$ are the respective (constant) group velocities. The interaction coefficients for deep-water gravity-capillary waves are given by McGoldrick (1965) and in their most perspicuous form by Simmons (1969) as

$$\gamma_s = -\frac{Jk_s}{4\omega_s}, \text{ (no sum)} \qquad J = \sum_{j=1}^{3} \omega_j \omega_{j+1} (1 + \mathbf{e}_j \cdot \mathbf{e}_{j+1}), \tag{13a,b}$$

in which $\mathbf{e}_j = \mathbf{k}_j/k_j$ and j is interpreted modulo 3. The three-wave equations of (12) have a rich structure (see Craik 1985 for a comprehensive discussion). They are an infinite-dimensional Hamiltonian system which is completely integrable (i.e. the Hamilton-Jacobi equation is separable), and they can be solved exactly for a wide class of initial data by the inverse scattering transform (see Kaup 1981 and the references cited there). In the absence of spatial gradients, they have exact solutions in terms of Jacobi elliptic functions (Ball 1964, Bretherton 1964), which exhibit periodic exchanges of energy among the three waves as well as the phenomenon of recurrence. There are a number of other exact solutions for special cases (e.g. see Craik 1985). Resonant triads occur on a time scale $t \sim t_0/\varepsilon$, in which t_0 is a characteristic waveperiod.

The equations for a single resonant quartet (Benney 1962, Bretherton 1964, Benney & Newell 1967) can be written in the compact form

$$(\partial_t + \mathbf{U}_s \cdot \nabla) A_s = iA_s \sum_{j=1}^{4} \gamma_{sj} |A_j|^2 + i\Gamma\omega_s A^*_{s+\delta} A_{s+2\delta} A_{s+3\delta}, \tag{14}$$

in which s is interpreted modulo 4; $\delta = +1$ for s odd; $\delta = -1$ for s even; and γ_{sj} and Γ are real-valued interaction coefficients. The interaction coefficients in the matrix (γ_{sj}) with $s, j = 1, 2, 3, 4$ are discussed by Phillips (1977, p. 85) for deep-water gravity waves; their form is given by Longuet-Higgins & Phillips (1962). These coefficients account for the nonlinear

dispersion of the waves with the diagonal terms corresponding to self interactions (Stokes 1847) and the off-diagonal terms corresponding to mutual interactions between wave pairs. The coefficient Γ accounts for energy exchange among the four waves; it is a complicated function of the frequencies and wavevector configuration of the underlying waves. An explicit expression for Γ in the general case has not been presented; however, Benney (1962) hints at its complexity and Longuet-Higgins (1962) gives an explicit result when (11) is satisfied with two coincident wavetrains (also see McGoldrick et al 1966). The four-wave equations of (14) have many interesting properties (see Craik 1985 for a review). They are not known to be integrable (Ablowitz & Segur 1981, p. 312), but exact solutions in terms of Jacobi elliptic functions exist when there are no spatial gradients (Bretherton 1964, Boyd & Turner 1978). Hence, as in the three-wave equations, periodic exchanges of energy among the wavetrains are possible. Resonant quartets occur on a time scale $t \sim t_0/\varepsilon^2$.

The elementary interactions described by the three- and four-wave equations are the backbone of RIT; their predictions and experimental validation are the primary basis for RIT's general acceptance. Yet, in many practical applications these equations are not sufficiently general, since a system that admits one resonant set of waves often admits many resonant sets simultaneously, as is the case for water waves.

MULTIPLE RESONANT INTERACTIONS When the underlying (linear) wavefield of (6a) comprises many waves—e.g. a discrete spectrum of S waves or a continuous spectrum—multiple and coupled resonances are often possible. A distinction is usually made between broad spectra and narrow spectra, since the latter enable some useful simplifications. In addition, the existence of multiple and coupled resonant sets among both broad and narrow spectra allows a choice between deterministic or stochastic descriptions. For broad spectra, stochastic descriptions dominate owing to the escalating complexity of deterministic descriptions and the absence of known initial conditions for systems like ocean waves. It should be noted also that the simplifying analyses[2] that result from adopting stochastic descriptions are purchased with assumptions on the nature of the underlying randomness; results can differ markedly with different assumptions. [Reviews of stochastic descriptions of water waves can also be found in Phillips (1977), West (1981), and Yuen & Lake (1982).]

[2] Simplification is obscured by the burdensome symbolism in many studies. We note the importance of symbolism in mathematics, e.g. see Whitehead (1958, p. 39) who cites the classical example of arithmetic-progress stalled until the arabic symbolism replaced the roman symbolism.

Broad-spectrum interactions Ablowitz & Haberman (1975a,b) used a deterministic approach with S large to study a general system with multi-triad resonances. They used the methods of Ablowitz et al (1974) to obtain a set of S integrable, nonlinear partial differential equations. These are coupled through M interlocked triads in which $M \geq (S-1)/2$. Ablowitz & Haberman (1975b) also considered the case of multiquartet interactions. The special case ($M = 2, S = 5$) of two resonant triads with one wavetrain in common was examined in the context of plasma waves by Wilhelmsson & Pavlenko (1973) [see also Weiland & Wilhelmsson (1977, p. 121)], who obtained exact solutions in terms of Jacobi elliptic functions—similar to the results for elementary interactions.

Stochastic descriptions of nonlinearly interacting water waves were pioneered by Hasselmann (1962, 1963a,b, 1966, 1967a) who recognized the special role of four-wave resonances for surface gravity waves and asserted the random-phase approximation or equivalently, asserted that wavefields are spatially homogeneous (and Gaussian). The random-phase assertion (RPA) is wrong for the multitriad or multiquartet descriptions of Ablowitz & Haberman (1975a,b). Whether it is right for resonant interactions among a broad spectrum of gravity or gravity-capillary water waves cannot be answered unequivocally. The RPA is plausible, and it appears useful in a practical sense for studying plasma waves (Davidson 1972, Section 13). In essence, the RPA relegates nonlinearity in four-wave resonances to acting on the slow time scale $t \sim t_0/\varepsilon^4$ whereas randomness acts on the faster time scale $t \sim t_0/\varepsilon^2$ (e.g. see Yuen & Lake 1982); hence, randomness dominates nonlinearity. The diminished nonlinearity allows energy transfers among resonant waves; however, the resonant set contains passive waves, which grow to a steady state, rather than active waves, which exchange energy periodically as in elementary resonant interactions. Thus, energy transfers are irreversible. For a discrete broad spectrum of underlying waves, Hasselmann's stochastic model yields an evolution (transport) equation for the spectral density of wave action per unit mass $N_1 := N(\mathbf{k}_1, t)$ with the form

$$\frac{\partial N_1}{\partial t} = \int_{-\infty}^{\infty}\int_{-\infty}^{\infty}\int_{-\infty}^{\infty} Q(\mathbf{k}_1,\mathbf{k}_2,\mathbf{k}_3,\mathbf{k}_4)\,[N_3N_4(N_1+N_2)-N_1N_2(N_3+N_4)]$$
$$\times\,\delta(\mathbf{k}_1+\mathbf{k}_2-\mathbf{k}_3-\mathbf{k}_4)\delta(\omega_1+\omega_2-\omega_3-\omega_4)\,d\mathbf{k}_2\,d\mathbf{k}_3\,d\mathbf{k}_4, \quad (15)$$

in which $Q(\mathbf{k}_1,\mathbf{k}_2,\mathbf{k}_3,\mathbf{k}_4)$ is a complicated interaction coefficient (see Webb 1978, for a succinct listing) and the Dirac delta functions select contributions only from resonant interactions. Not only is the content of (15)

difficult to see, it is difficult to calculate. Rough calculations using (15) and (JONSWAP) oceanic data (Sell & Hasselmann 1972, Hasselmann et al 1973 as referenced by Phillips 1977, p. 139) indicated that energy flows toward a broad spectral peak, but the results were inconclusive (Phillips 1977, p. 138). More well-founded calculations using (15) and a broad spectrum by Webb (1978), Masuda (1981, 1986), Hasselmann & Hasselmann (1985), and Hasselmann et al (1985) also showed, among other things, that energy flows toward a broad spectral peak from high wavenumbers. More recent calculations by Resio & Perrie (1991) affirmed this result and examined energy fluxes among spectral regions for a variety of spectral parameters.

Valenzuela & Laing (1972), Holliday (1977), and van Gastel (1987a) used a stochastic model similar to Hasselmann's to study a broad discrete spectrum of gravity-capillary waves, in which resonant triads occur. Van Gastel (1987a) gives an especially perspicuous derivation of the transport equations, which she writes in terms of the variance density G according to

$$\frac{\partial G_1}{\partial t} = \frac{k_1}{16\pi\omega_1} \int_{-\infty}^{\infty}\int_{-\infty}^{\infty} J^2(\mathbf{k}_1, \mathbf{k}_2, \mathbf{k}_3)\left[\frac{k_1}{\omega_1} G_2 G_3 - \frac{k_2}{\omega_2} G_3 G_1 - \frac{k_3}{\omega_3} G_1 G_2\right] \times \delta(\mathbf{k}_1 - \mathbf{k}_2 - \mathbf{k}_3)\delta(\omega_1 - \omega_2 - \omega_3)\, d\mathbf{k}_2\, d\mathbf{k}_3. \quad (16)$$

[The relation between the variance density G in (16) and wave action density per unit mass N in (15) is discussed by van Gastel (1987b).] The interaction coefficients J^2 that appear in the stochastic model of (16) are proportional to the square of those in the deterministic model of (12) and (13) for an elementary resonant triad. A similar revealing connection between the interaction coefficients for gravity waves in the stochastic model of (15) with those of the deterministic elementary resonant quartet of (14) has not been found. Van Gastel (1987a) also used calculations to show that nonlinear interactions caused energy to flow away from a broad spectral peak toward wavenumbers larger than that of Wilton ripples [$k_0 = (\varrho g/2T)^{1/2}$]. In her stochastic model the interactions within a resonant triad were independent of other triads. The time scale of randomness was $t \sim t_0/\varepsilon$, whereas the time scale of nonlinearity was $t \sim t_0/\varepsilon^2$.

The effects of spatial inhomogeneities for a broad spectrum of waves were investigated by Willebrand (1975) who estimated that they are small in deep water, but the arguments are subtle. Watson & West (1975) developed a stochastic model that included specific external mechanisms to account for spatial inhomogeneities ab initio. They showed that nonresonant interactions between these mechanisms and the wavefield were important. A general stochastic model for a broad continuous spectrum

of waves which did not use the RPA was presented by Benney & Saffman (1966) and Benney & Newell (1969). Their analyses made essential use of the smoothness of the underlying wave spectrum; hence, their results cannot be compared directly with the discrete spectral results, in which the spectrum is a sum of Dirac delta functions. Segur (1984) suggested that this smoothness amounts to enhancing linear dispersion relative to nonlinear coupling so that their model applies in a different regime from those of elementary resonant interactions and Hasselmann's model. Segur (1984) developed a stochastic model—which did not use the RPA—for coupled, resonant triads of interacting, localized wave packets. His derivation closely paralleled Boltzmann's derivation for a dilute gas of interacting molecules (kinetic theory), but important differences arose in consequence of fundamental differences between interacting molecules and interacting wave packets. In particular, two interacting wave packets generate a third ab initio so that the essential assumption of a dilute system was eventually violated. Segur's final evolution equation for the probability density of finding a particular wave packet at a particular time and location in phase space differed considerably from Boltzmann's equation for dilute gases. Segur suggested that his model probably does not have stable equilibrium solutions, which play a central role in the kinetic theory of gases.

Narrow-spectrum interactions When the wavefield has a narrow spectrum and four-wave resonances are the first to occur, expansions about the dominant wavetrain reduce both deterministic and stochastic descriptions to simpler forms. [In terms of (11a), the wavevectors of a narrow spectrum are nearly collinear and nearly equal in magnitudes.] Benney & Roskes (1969), Davey & Stewartson (1974), Djordjevic & Redekopp (1977), and Ablowitz & Segur (1979; 1981, p. 317) exploited the spectrum's narrowness deterministically. They obtained (dimensionless) evolution equations in terms of the complex amplitude A with the form

$$iA_t+\zeta A_{xx}+\mu A_{yy} = \chi|A|^2A+\chi_1\Phi_xA, \tag{17a}$$

$$\beta\Phi_{xx}+\Phi_{yy} = -\beta_1(|A|^2)_x, \tag{17b}$$

in which the coefficients ζ, μ, χ, χ_1, β, and β_1 are functions of the dominant wavetrain (see the aforementioned references or Perlin & Hammack 1991), Φ is a velocity potential for the mean flow that is induced by the wavefield, and the spatial coordinates are referenced to a frame moving with the wavetrain at its group velocity. [We also require that $(kh)^2 \gg \varepsilon$ to avoid shallow water.] Equations (17), which are often termed the Davey-Stewartson equations, assume that the dominant wavetrain propagates mainly in the x-direction, i.e. its wavevector is, say, $\mathbf{k} = (l_0, 0)$. These

equations have many interesting variations. For example, in the deep-water limit ($kh \to \infty$) the mean flow disappears yielding

$$iA_t + \zeta A_{xx} + \mu A_{yy} = \chi |A|^2 A, \tag{18}$$

which was first derived by Zakharov (1968) and, according to Ablowitz & Segur (1981, p. 322), is probably not solvable by the inverse scattering transform. Equation (18) can also be derived directly from the four-wave equations (Phillips 1981a). The mean flow and amplitude equations in (17) decouple when either the transverse (y) variations are neglected to obtain

$$iA_t + \zeta A_{xx} = \chi |A|^2 A, \tag{19}$$

or when the longitudinal (x) variations are neglected to obtain

$$iA_t + \mu A_{yy} = \chi |A|^2 A. \tag{20}$$

Both (19) and (20) are nonlinear Schroedinger (NLS) equations, first derived for longitudinal modulations by Benney & Newell (1967), Zakharov (1968), and Hasimoto & Ono (1972). [A comprehensive review of NLS equations in the context of water waves is given by Peregrine (1983).] These equations are completely integrable and solvable by the inverse scattering transform (Zakharov & Shabat 1972). In particular, (19) predicts the Benjamin & Feir (B-F, 1967) instability of a wavetrain to longitudinal, modulational (sideband) perturbations and also models the instability's long-time evolution. The B-F instability occurs when $\zeta\psi < 0$; the unstable wavenumbers lie in longitudinal sidebands $l_0 \pm \delta l$, in which $\delta l = |A_0|(-2\psi/\zeta)^{1/2}$ and $|A_0|$ is the initial amplitude of the underlying wavetrain. Comprehensive reviews of (18) and (19), the B-F instability, and its long-time behavior, as well as experimental and numerical results are presented by Yuen & Lake (1980, 1982), and we discuss them in more detail subsequently. In a little noticed paper, Phillips (1967) showed that the B-F instability could be obtained directly from the four-wave equations for gravity waves. Importantly, his results showed that the B-F instability of gravity waves is possible for longitudinal and transverse sideband modulation, i.e. for oblique wavetrain perturbations.

Equation (20) is a nonlinear Schroedinger equation for a wavetrain that propagates in the x-direction but is modulated in the transverse y-direction; it is commonly used in wave diffraction studies (e.g. Zakharov & Shabat 1972). Perlin & Hammack (1991) used (20) to study transverse sideband instabilities of gravity-capillary wavetrains. When $\mu\chi < 0$ in (20), a wavetrain with wavevector $\mathbf{k} = (l_0, 0)$ is unstable to wavevectors $\mathbf{k} = (l_0 \pm \delta m)$, in which $\delta m = |A_0|(-2\chi/\mu)^{1/2}$. According to this result, all wavetrains with wavenumbers $k > k_0 = (\varrho g/2T)^{1/2}$, i.e. wavenumbers greater than that of Wilton ripples, have unstable sidebands of transverse

wavenumbers while those with $k < k_0$, which includes gravity waves, do not. Moreover, Perlin & Hammack (1991) showed that, according to (19) and (20), the growth rates of the most unstable longitudinal and transverse modes are equal. A more general result for gravity waves was obtained by Hayes (1973), Davey & Stewartson (1974), Alber (1978), and Martin & Yuen (1980, repeated in Yuen & Lake 1980, 1982) who performed a linear stability analysis directly on (17), (18), or their equivalent. They found an unbounded band of oblique wavetrain perturbations with both transverse and longitudinal wavenumbers that destabilized the wavetrain. [This result is consistent with that of (20) when the longitudinal perturbation wavenumber vanishes.] However, as noted by Martin & Yuen (1980), this unboundedness introduced perturbations which violated the narrow-spectrum approximation that underlies (17) and (18). This violation led Crawford et al (1981a) to abandon (17) and its variations in favor of a less restrictive model equation.

Crawford et al (1981a) investigated the Zakharov integral equation (Zakharov 1968):

$$\frac{\partial B_1}{\partial t} = \int_{-\infty}^{\infty}\int_{-\infty}^{\infty}\int_{-\infty}^{\infty} T(\mathbf{k}_1, \mathbf{k}_2, \mathbf{k}_3, \mathbf{k}_4) B_2^* B_3 B_4 \delta(\mathbf{k}_1 + \mathbf{k}_2 - \mathbf{k}_3 - \mathbf{k}_4) \times e^{i\Delta\omega}\, d\mathbf{k}_2\, d\mathbf{k}_3\, d\mathbf{k}_4, \quad (21)$$

in which $B(\mathbf{k}, t)$ is a complex envelope spectral function, T is an interaction coefficient, and $\Delta\omega = \omega_1 + \omega_2 - \omega_3 - \omega_4 = O(\varepsilon^2)$ accounts for slight detuning of the resonance conditions. Strictly speaking, (21) is not restricted to a narrow spectrum, rather it requires that the spectrum have dominant components that lie within a bandwidth of $O(\varepsilon^2)$ around the resonant curves of (11). When the resonance conditions of (11) are satisfied exactly, the four-wave equations are recovered. The B-F instability can be studied utilizing the detuning in (21). Results show that gravity waves are unstable to oblique wave perturbations and that the band of unstable wavenumbers is bounded. Importantly, the most unstable perturbation occurs when the transverse wavenumbers vanish so that the classical longitudinal B-F instability is dominant. A comprehensive review of (21) and further results are given in Yuen & Lake (1980, 1982).

Stochastic descriptions for narrow spectra received a major impetus from Longuet-Higgins (1976) who used Equation (18) as a starting point, assumed a discrete spectrum of waves with uncorrelated phases (i.e. the random phase assertion), and averaged and summed over time to obtain Hasselmann's Equation (15) with an explicit expression for the interaction coefficient, $Q(k, k, k, k) = 4\pi k^6$, in which k is the magnitude of the dominant wavevector. Fox (1976) used this result and (JONSWAP) oceanic

data to perform computations with (15). His results differed markedly from the earlier computations by Sell & Hasselmann (1972); he found that energy flows away from, instead of toward, the spectral peak. Dungey & Hui (1979) improved Longuet-Higgins (1976) result by accounting for the finite spectral width of the narrow spectrum and showed that the flow of energy away from the spectral peak decreases as a consequence of its finite width. Masuda (1981, 1986) clarified these varying results using (15) without approximating the interaction coefficient Q for spectral shape. His well-founded computations showed that although energy does flow away from the peak in a broad spectrum, it flows toward a peak in a narrow spectrum. Moreover, Masuda found that in a spectrum with both low- and high-frequency peaks, the energy exchanges occurred such that the high-frequency peak was reduced and the low-frequency peak was intensified. Resio & Perrie (1991) also examined the effects of spectrum peakedness on energy fluxes within the spectrum. All of these results for gravity waves were consistent with van Gastel's (1987a) results for gravity-capillary waves.

Yuen & Lake (1982) started with the Zakharov integral Equation (21) and derived a stochastic model which did not use the RPA. The resulting wavefield comprised modulations (spatial inhomogeneity) with a time scale $t \sim t_0/\varepsilon^2$ while nonlinear interactions (energy exchange) occurred on a time scale $t \sim t_0/\varepsilon^4$ as in (15). Crawford et al (1980) used this stochastic model to test the stability of a narrow, homogeneous spectrum to inhomogeneous disturbances. They found a band of perturbation wavenumbers to which the narrow homogeneous spectrum was unstable; the bandwidth depended inversely on the strength of randomness. As the randomness approached zero they recovered the B-F instability; as randomness increased, the B-F instability diminished and finally disappeared so that the spectrum was stable. Alber (1978) obtained similar results beginning with (17). Janssen (1983b) studied the long-time behavior of an unstable sideband mode for varying degrees of randomness. He found that the sideband's spectral amplitude initially overshot and then oscillated in a damped manner to its long-time value. Both the overshoot and damped oscillations disappeared as the width of the homogeneous spectrum increased.

HIGHER-ORDER RESONANT INTERACTIONS Dysthe (1979) extended the nonlinear Schroedinger equation (NLS) for gravity waves to $O(\varepsilon^4)$ and found that the mean flow, which is a degenerate wave, varies as a consequence to wavetrain modulations. The higher-order NLS equation predicted a large but bounded band of unstable oblique wave perturbations, and, similar to the results of Crawford et al (1981a) for the Zakharov equation, it predicted that the most unstable perturbations for gravity waves are

collinear. Calculations using this model for collinear perturbations by Lo & Mei (1985) showed good agreement with Keller's experimental data, which is (only) reported there. Further calculations by Lo & Mei (1987) using oblique perturbations showed that the higher-order NLS did not lead to a basic violation of its narrow-band approximation as (18) did. Janssen (1983a) used Dysthe's higher-order NLS equation to study a random field of gravity waves with the random phase approximation and recovered the results of Dungey & Hui (1979).

Hogan (1985, 1986) extended the Zakharov equation to $O(\varepsilon^4)$ for a narrow spectrum of gravity-capillary waves. Stiassnie (1984) showed that the higher-order NLS equation could bc obtained as a special case of the Zakharov equation. Stiassnie & Shemer (1984) extended the Zakharov equation for gravity waves to include quintet interactions. Their calculations for wavetrain stability were qualitatively similar to more exact results of McLean (1982a,b) who used direct computations of the unapproximated (Euler) equations. Stiassnie & Shemer (1987) used the higher-order Zakharov equation to study the coupled evolution of resonant quartets and resonant quintets, which lead to the instability of deep-water gravity wavetrains.

SUMMARY COMMENTS ON RIT In summary, we emphasize several aspects of RIT whose importance will be clearer in the subsequent comparisons of theoretical and experimental results. First, RIT is a perturbative description which supposes wave-wave interactions are weak. Hence, RIT depends crucially on the existence of a single small parameter ε, regardless of the number of wavetrains involved. Second, RIT neglects nonresonant interactions, which are those excluded by kinematical considerations, i.e. by Equations (10) and (11), and those that satisfy kinematical conditions but are excluded by dynamical considerations. There is experimental evidence to suggest that caution be used before neglecting dynamically nonresonant interactions (Perlin et al 1990). Third, most of the discussion herein has assumed that the wavetrains satisfy the resonance conditions exactly. Precise tuning is not necessary and detuning is easily incorporated into RIT (e.g. see Craik 1985) as it was in (21). Fourth, the RIT presented herein neglects water viscosity, although the weak viscous effects that are typical of water waves may be significant, especially over the long time scales associated with the weak interactions of RIT. Weak viscosity accounts for three important effects in experiments: It attenuates wavetrain amplitudes, it detunes resonances, and it imposes a minimum ε in order for the growth of inviscid instabilities to occur. All of these effects are easily incorporated into RIT. For example, Miles (1984a,b) noted that the effects of weak (linear) viscosity are included in nonlinear evolution

equations by letting $\partial/\partial t \rightarrow \partial/\partial t + \beta$, in which β is a viscous damping rate which usually varies among wavetrains. A comprehensive discussion of resonant interactions in systems that do not conserve energy can be found in Craik (1985, 1986); also see Craik & Moroz (1988) and Murakami (1987).

RESONANT INTERACTION EXPERIMENTS

In the previous section we reviewed some of the theoretical literature in which the special role of resonant interactions provided the framework for analysis. In this section we review the experimental literature in which there are measurements that allow us to test the predictions of RIT, either qualitatively or quantitatively. We begin by reviewing experiments that address the applicability of Kelvin's linear dispersion relation for water waves on a free surface. This dispersion relation is crucial to all applications of RIT, and it has an interesting history of experimental verification which illustrates the difficulties of measuring wavevectors on a two-dimensional water surface. Then we review resonant interaction experiments for gravity waves, gravity-capillary waves, and capillary waves.

Wave Dispersion on a Water Surface

DISPERSION RELATION AND WAVE CLASSIFICATION Kelvin[3] (1871) obtained the dispersion relation for infinitesimal wavetrains ($\varepsilon \rightarrow 0$) on the free surface of an inviscid water layer with constant density ϱ, constant surface tension T, quiescent depth h, and gravitational force per unit mass g, i.e.

$$c_2 = \frac{\omega^2}{k^2} = \frac{g}{k}(1+\tau)\tanh kh. \tag{22}$$

Here c is defined as the wave celerity and $\tau = Tk^2/\varrho g$ measures the relative importance of surface tension and gravitation, and resembles a reciprocal Bond number. To avoid shallow water we take $kh \gg 1$ so that the relevant perturbation parameter is the wave steepness $\varepsilon = ak$. Wilton (1915) showed that there is a countably infinite family of internal resonances among surface waves corresponding to wavetrains with $\tau = 1/n$, $n = 2, 3, \ldots$. With the values $T = 73$ dyn/cm, $\varrho = 1$ gm/cm^3, and $g = 980$ cm/s^2, second-harmonic resonance occurs at $\tau = 1/2$ for a wavetrain with $f = \omega/2\pi = 9.8$ Hz, third-harmonic resonance occurs at $\tau = 1/3$ for a wavetrain with $f = 8.4$ Hz, and so on. It is convenient to use (22) and the theoretical results for resonant triads and quartets (modulational instabilities) reviewed in

[3] Kelvin did not consider the effects of finite depth, which we have included in (22), but he did include the effects of air density, which we have neglected.

the previous section to define the following (distinct) frequency ranges for classifying surface waves. We define gravity wavetrains as those with $\tau < 0.155$, which corresponds to $f < 6.4$ Hz. Wavetrains in this frequency range are modulationally unstable with collinear wave perturbations being dominant (Djordjevic & Redekopp 1977, Crawford et al 1981a). (Note that the group velocity of water waves is minimum for $f = 6.4$ Hz.) We define capillary wavetrains as those with $\tau > 2.0$, which corresponds to $f > 19.6$ Hz; resonant triads are possible in this frequency range (Simmons 1969). (Note that $f = 19.6$ Hz is the second harmonic of Wilton ripples.) We define gravity-capillary waves (or ripples) as those with $6.4 < f < 19.6$ Hz. Waves in this frequency band are predicted to have three types of weakly nonlinear behavior. Wavetrains with $6.4 < f < 9.8$ Hz are stable to modulational instabilities (Hogan 1985, Djordjevic & Redekopp 1977); however, five members of the family of Wilton ripples ($n = 2$–6) are embedded in this band. Wavetrains with $f > 9.8$ Hz are modulationally unstable to collinear and oblique wavetrain perturbations (Perlin & Hammack 1991). All of these resonances and wave classifications are summarized in Figure 1.

DISPERSION RELATION EXPERIMENTS Fundamental to the application of RIT is the accuracy of the linear dispersion relation; yet, experimental verification of (22) is deceivingly difficult. Von Matthiessen (1889) first conducted experiments to test the validity of Kelvin's Equation (22) using a porcelain basin and a variety of liquids. He used two tuning forks with attached dippers to excite two wavetrains with circular wavecrests; the frequency range was 8.4–1024 Hz for experiments using distilled water. Von Matthiessen used two procedures to measure wavelengths. First, he counted the number of wave crests in the standing wavefield between the two tuning forks, which were separated by a known distance. Second, he measured wavelengths of the progressing waves to either side of the tuning forks by examining reflections of wavefield images on the polished tuning fork. (Presumably, he used an intermittent light source to render the images stationary, but the details are unclear to us.) Von Matthiessen used a standard value (73 dyn/cm) for surface tension in calculating predicted wavelengths with (22). Errors between predicted and measured wavelengths ranged between 0–12% with a mean error of 3.6%. We note that von Matthiessen's lowest measurement frequency (8.4 Hz) corresponds to the third-harmonic resonance. He observed that more crests occurred than expected for this wavetrain (only), undoubtably resulting from internal resonance, which was unknown at his time.

Rayleigh (1890) indirectly tested the validity of (22) using more refined experiments in his efforts to measure surface tension on clean and greasy

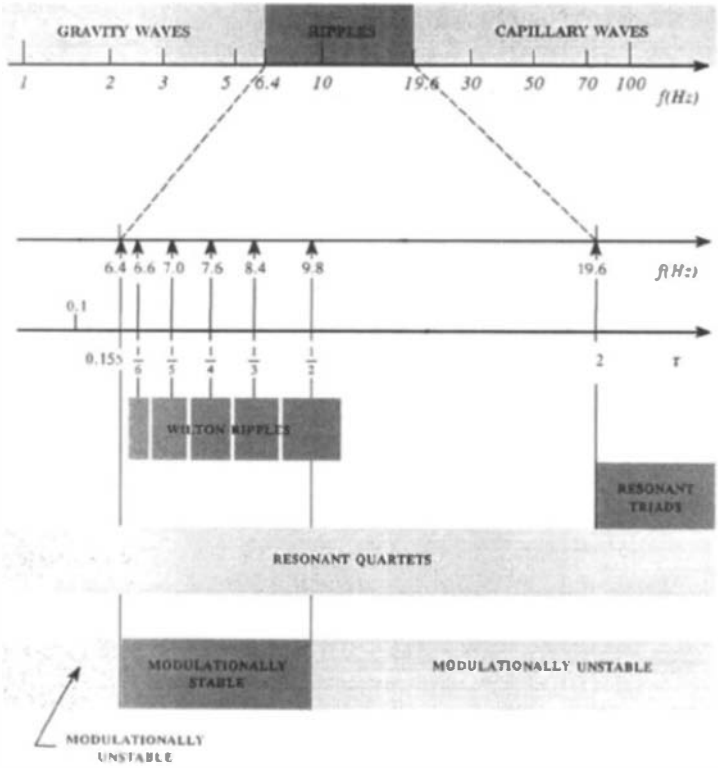

Figure 1 Surface wave classification in terms of frequency f and dimensionless surface tension τ based on weakly nonlinear wavetrain instabilities.

water surfaces. He used a 12 in × 12 in basin filled with either tap or distilled water, and cleaned the surface using an expandable brass hoop which pushed impurities aside. Like von Matthiessen, Rayleigh used tuning forks to generate waves, but unlike von Matthiessen, he used a 2.5 in glass plate as a paddle so as to generate plane waves. His wave amplitudes were so small that they could not be seen with the unaided eye. Rayleigh observed them using an optical arrangement comprised of a light source (a small gas flame) located in the focal plane of a large (6 in diameter) lens, which was located just above and parallel to the water surface. An image was formed on a screen by light after double passage through the lens; this image was rendered stationary by making the light source intermittent with a plate in front of the light which vibrated isoperiodically with the tuning fork used to generate waves. Rayleigh calibrated image lengths by viewing a bar of known dimension situated in close proximity to the water

surface. He estimated that his measurements were in error by less than 1%. Using wave frequencies of 42.12 and 124.9 Hz, Rayleigh found that the mean tension of a clear surface was 74.2 and 73.6 dyn/cm, respectively, which indicated a discrepancy of about 1%. This "method of ripples" which Rayleigh used for measuring surface tension (at the suggestion of P. G. Tait) remains a standard method today (Freundlich 1922, p. 15; Adamson 1990, p. 40).

It is testimony to the difficulty of such experiments, and perhaps Rayleigh's influence, that further controlled experiments to verify (22) apparently were not reported until 1955 by Dobroklonskii. According to Scott (1981), Dobroklonskii used careful procedures which included continual renewal of the water surface in order to keep it clean. Dobroklonskii examined waves in the frequency range of 12–200 Hz and obtained good agreement with (22).

Davies & Vose (1965) examined the accuracy of (22) for capillary waves on water surfaces that were clean and on water surfaces that were covered with monomolecular films. They generated waves with frequencies of 50–920 Hz in a small glass tank (the size was not given) using a glass paddle driven horizontally by an electromagnetic mechanism; frequencies were carefully monitored. They cleaned the glass with chromic acid followed by washings with phosphoric acid, tap water, and distilled water. They cleaned water surfaces by spreading talc which was subsequently vacuumed. Surface tension was continually monitored with a du Nouy tensiometer. Like Rayleigh, Davies & Vose measured wavelengths using an optical arrangement and stroboscopic light source. Their experiments showed Kelvin's equation to be accurate to within 1.5% for clean surfaces over the entire frequency range. Unfortunately, they encountered (unspecified) experimental difficulties when measuring wavelengths on surfaces with insoluble films which precluded definitive results. Nevertheless, they described Kelvin's equation as approximately valid when films exist. (We note that the dispersion relation depends weakly on the viscoelastic properties of a surface film, e.g. see Levich 1962, p. 613 or Cini & Lombardini 1978.)

Scott (1981) examined surface waves with frequencies of 2–10 Hz using the extraordinary measures of Davies & Vose (1965) in a larger 9.5 cm × 100 cm basin in which the water depth was 2.9 cm. Scott used wetted, ground glass sidewalls, which were cleaned similarly to the procedures of Davies & Vose (1965), in order to maintain a static contact angle of zero and minimize edge effects. He used doubly distilled water, and vacuumed the water surface before each experiment. Scott generated waves at one end of the channel using a vertically oscillating wedge whose frequency was carefully monitored. He used a nonintrusive proximity gauge to measure

passing waves, and measured wavelengths with an accuracy of $\pm 0.4\%$ by traversing the wavefield at known distances and number of wavelengths. The mean deviation between measured and predicted wavelengths in Scott's experiments was 1.3%; this deviation arose mainly from the higher-frequency waves.

Henderson & Lee (1986) conducted experiments in a 91 cm $\times$ 30 cm wave channel; the water depth was 2.54 cm. They generated wavetrains in the range of 6–20 Hz using a vertical plate hinged at the bottom and pushed horizontally at the top by an electromagnetic servomechanism. They measured wavelengths by traversing the wavefield with an in situ gauge at known distances and number of wavelengths. They used doubly distilled water and special cleaning procedures but did not employ the extreme measures of either Davies & Vose (1965) or Scott (1981) to clean the water surface. (Undoubtably, films were present on their surfaces.) Nevertheless, Henderson & Lee obtained excellent agreement between measured and predicted wavelengths using $T = 73.0$ dyn/cm in (22) when the water was filtered of particles with nominal sizes larger than 0.2 μm. When the water was not filtered of particles, a value of $T = 54.0$ dyn/cm in (22) gave similar agreement between predicted and measured data. The special role of particulate contamination does not appear to have been noticed previously, although it might be responsible for Rayleigh's observation that on occasion distilled water proved less satisfactory than tap water. (Typically, the distilling process does not remove small particles.)

The experimental difficulties in measuring frequencies and wavelengths for simple wavetrains are greatly increased when wavefields comprise many wavelengths and directions of propagation. Yet, such measurements are crucial in distinguishing between waves that arise from resonant interactions, which satisfy (22), and those that arise from nonresonant interactions, which don't satisfy (22). This measurement difficulty may account for the curious and potentially damning (as regards the application of RIT) results for wind wavefields obtained by numerous investigators beginning with Ramamonjiarisoa & Coantic (1976) who used two, in situ, wave gauges and filtered space-time correlations to obtain $c(k)$. [See Yuen & Lake (1982) for a discussion and a list of references; also see Ramamonjiarisoa & Mollo-Christensen (1979, 1981) and discussions by Huang (1981), Komen (1980), and Papadimitrakis (1986).] Measurements indicated that the phase speeds of waves with frequencies greater than that of the dominant wavetrain were constant—departing significantly from the predictions of (22). Crawford et al (1981b) attributed these departures to nonlinearity and spectral bandwidth. Huang & Tung (1977) and Longuet-Higgins (1977) attributed them to directional effects. Phillips (1981b) argued that these departures were due primarily to convection by the

orbital velocities of the dominant (long) waves, and were thus a manifestation of the measurement technique. Plant & Wright (1979) used Doppler radar measurements of a wavefield, which avoid some of the inherent problems in two-probe correlation techniques, and found that the high-frequency waves dispersed according to (22). Gotwols & Irani (1980) used optical remote sensing measurements of the ocean surface and found excellent agreement between (22) and measured phase speeds. Barrick (1986) examined the role of (22) in radar measurements and concluded that (22) and Phillips' (1981b) appraisal were correct. Melville (1983) used measurements with two in situ gauges and an envelope-detection data analysis to find that (22), suitably modified by the Stokes' (1847) correction for large wave steepnesses, was accurate for strongly modulated wavetrains.

Gravity-Wave Experiments

The first comparisons between the predictions of resonant interaction theory and gravity-wave measurements were reported in companion papers by Longuet-Higgins & Smith (1966) and McGoldrick et al (1966). Both experiments were designed according to a suggestion by Longuet-Higgins (1962) in which (11) has the form $\mathbf{k}_1+\mathbf{k}_2 = 2\mathbf{k}_3$ and $\omega_1+\omega_2 = 2\omega_3$. Both Longuet-Higgins & Smith and McGoldrick et al generated waves *2* and *3* with two orthogonal wavemakers along adjacent basin walls; beaches were located along opposing walls to minimize reflections. They obtained continuous time signals of the water-surface displacements with in situ wave gauges at different distances from the wavemakers. They processed these signals with a sharply tuned, band-pass filter with variable center frequency so as to obtain amplitude-frequency spectra. They examined the spectral amplitudes at different gauges in order to obtain the spatial growth/decay rates of nascent/generated waves. According to the four-wave equations (14), wave *1* should be generated ab initio by resonant energy transfers from waves *2* and *3*; theoretical predictions of its growth rate which accounted for detuning were obtained using the four-wave equations. Their measured spectra contained large peak amplitudes at frequencies of the generated waves, and small peak amplitudes at frequencies of superharmonics and many sum-and-difference frequencies that included $\omega_1 = 2\omega_3-\omega_2$. In each spectrum, the spectral amplitude at ω_1 exceeded that of superharmonic and other sum-and-difference frequencies, suggesting that it resulted from a resonant rather than nonresonant interaction. More convincingly, comparison of spectral amplitudes at different gauge sites showed that, unlike all other spectral peak amplitudes, the amplitudes at ω_1 grew linearly with distance as predicted by RIT. Moreover, the measured growth rates were 20% higher

than those predicted by RIT, which did not account for viscous attenuation. These experimental results firmly established the special role of resonant interactions.

The discovery of the modulational instability of a Stokes gravity wavetrain evolved from theoretical studies by Lighthill (1965) and Whitham (1967) and culminated with the definitive study by Benjamin & Feir (1967), who were strongly motivated by Feir's laboratory experiments. [Zakharov (1968) also discovered this instability theoretically, but his terse paper was unnoticed in the West until sometime later.] Unfortunately, Benjamin & Feir did not give a detailed report of their experiments as they originally intended (Benjamin & Feir 1967), although Benjamin (1967) did give a brief report. Benjamin & Feir generated wavetrains at one end of a long tank using a mechanically operated paddle whose motion was either regular or modulated to generate collinear wavetrains at the predicted most-unstable sideband frequencies. (The experiments were conducted in two facilities.) They used in situ wave gauges along the channel to obtain continuous time signals for the vertical motion of the water surface. They obtained modulational periods and sideband growth rates directly from wave-gauge records and from spectral analyses. Their measured modulational periods agreed well with those predicted. Their measured growth rates agreed qualitatively with those predicted; however, even when the effects of viscous damping were considered, predicted growth rates were nearly twice those measured. Lake & Yuen (1977) reexamined the data of Benjamin (1967) and attributed the large discrepancies to inappropriate values for the steepnesses of generated waves, which did not have the proper shape of Stokes waves. Lake & Yuen (1977) corrected the growth rates measured by Benjamin and obtained good agreement with predictions. Longuet-Higgins (1978b) used the original data of Benjamin and found better agreement with his theoretical results that accounted for finite-amplitude effects on growth rates. Regardless of refinements to measurements or theoretical predictions, Benjamin's & Feir's pioneering experiments showed unequivocally that deep-water, gravity wavetrains are unstable to modulations that result from collinear, resonant-quartet interactions with waves of nearly the same (sideband) frequencies.

In spite of the excitement and interest caused by the discovery of the Benjamin-Feir instability, ten years passed before additional laboratory experiments on the instability and long-time evolution of a deep-water gravity wavetrain were reported by Lake et al (1977). Lake et al were motivated in part by interest in the nonlinear Schroedinger equation and its exact solution for localized initial data by the inverse scattering transform. [Related experiments on deep-water wave packets were reported by Feir (1967) and Yuen & Lake (1975).] They generated wavetrains with fre-

quencies of 1–5 Hz using a wavemaker, driven by a programmable servomechanism, located at one end of a 40 ft tank which contained a beach for absorbing wave energy at the opposite end. They used a linear array of in situ wave gauges along the wave channel to measure water surface motion. The continuous time signals from these gauges were recorded on FM tape for subsequent playback to an analog power-spectrum analyzer. Most of the experimental wavetrains had steepnesses in the range $0.10 \leq \varepsilon \leq 0.35$; wave breaking occurred for the steepest wavetrains. As expected, the wavetrains were unstable to sideband frequencies, and the measured, initial spatial growth rates agreed well with predictions. By exploiting the control available in these experiments, Lake et al were able to generate wavetrains with the same amount of sideband amplification that they measured at the gauge site farthest from the wavemaker. In this manner they effectively observed wavetrain evolution over much longer distances than their tank length. These long-time measurements showed preferential growth of the lower (frequency) sideband; this asymmetry is not predicted by either the Benjamin-Feir analysis or the nonlinear Schroedinger equation. Lake et al also found that the growth of modulations eventually ceased, followed by a period of demodulation and near recurrence of the original wavetrain. However, at recurrence, most of the energy resided in a wavetrain at the lower sideband frequency. An unequivocal explanation for this frequency downshift has not been established, but it seems to be related to strongly nonlinear effects such as wave breaking. (For example, see Melville 1982, 1983; Su et al 1982; Janssen 1983a; Hatori & Toba 1983; Trulsen & Dysthe 1990; Hara & Mei 1991.)

Melville (1983) conducted experiments in a wave channel that was 28 m $\times$ 50 cm and filled with water to a depth of 60 cm. He generated 2-Hz wavetrains with large steepnesses ($0.23 \leq \varepsilon \leq 0.29$) using a paddle driven by a hydraulic servomechanism. A beach, which began 16 m from the paddle, was used to dissipate wave energy. Melville measured the motion of the water surface using two in situ wave gauges located 8 cm apart and obtained discrete time signals at frequencies of 100- and 200-Hz. He used a Hilbert transform (envelope detection) technique to process these signals which, unlike spectral techniques, rendered temporal information on frequency, wavenumber, and phase-speed modulation. Melville found that the dispersion relation (22) was accurate for gravity waves when modified to account for weak nonlinearity (Stokes 1847). He also found that very rapid variations in wave phase occurred near minima in the wavetrain's envelope; these phase jumps were similar to the "crest pairing" described by Ramamonjiarisoa & Mollo-Christensen (1979). (Coalescence of wave crests is a possible explanation for the frequency downshift mentioned above.) Melville (1982) examined large-amplitude wavetrains and found

two distinct regions of behavior. For $\varepsilon \leq 0.29$ wavetrain evolution remained (sensibly) two-dimensional and the Benjamin-Feir instability was dominant; asymmetric sideband growth occurred subsequent to wave breaking. For $\varepsilon \geq 0.31$, the wavetrains became three-dimensional and the Benjamin-Feir instability was no longer dominant. Melville's experiments and his nontraditional data analysis provided new insight into the richness of the Benjamin-Feir instability whose qualitative features persisted for wave amplitudes well outside the putative range of validity of four-wave interaction theory.

Su et al (1982), Su (1982), and Su & Green (1984) reported experiments on deep-water gravity waves performed in two large experimental facilities: a 137.2 m × 3.7 m × 3.7 m tank and a 340 m × 100 m × 1 m (outdoor) basin. They used mechanical, plunger-type wavemakers, one that spanned the 3.7 m tank width and one that spanned 15.8 m of the 100 m basin width. Su et al (1982) and Su (1982) generated wavetrains with frequencies of 1.05–1.55 Hz and large steepnesses of $0.16 \leq \varepsilon \leq 0.34$ which led to breaking. They observed a fascinating sequence of instabilities in these large-amplitude, long-crested deep-water wavetrains which were measured with in situ wave gauges and photographic records. They interpreted their measurements within the framework of normal-mode instabilities calculated by Longuet-Higgins (1978a,b) and McLean (1982a) and within the framework of wavetrain bifurcations calculated by Meiron et al (1982). These calculations were based on the unapproximated (Euler) equations; hence, their results are not directly within the purview of RIT; nevertheless, the qualitative features of McLean's calculations were obtained by Stiassnie & Shemer (1984, 1987), who used a perturbative approach to extend the Zakharov equation to include resonant quintets. RIT supposes a time-scale separation between resonant quartets and quintets which was not evident in the measurements of Su and coworkers for large-amplitude wavetrains. Instead, they observed that a two-dimensional wavetrain near the wavemaker evolved quickly into a three-dimensional wavetrain of spilling breakers followed by another transition to a modulated two-dimensional wavetrain with a lower steepness and frequency. Although these results are only tenuously interpreted in terms of RIT, it is noteworthy that Su and coworkers found that large-amplitude bifurcated wavetrains exhibited the Benjamin-Feir instability.

Su & Green (1984) conducted experiments on deep-water gravity wavetrains with a single frequency of 1.23 Hz and steepnesses of $0.09 \leq \varepsilon \leq 0.20$ using the tank described above and a linear array of ten in situ wave gauges along the tank. They observed the following pattern of wavetrain evolution. The Benjamin-Feir instability [resonant quartets or the "Type I" instability of McLean (1982a,b)] developed gradually

at first, but then grew more rapidly causing intense modulations of the wavetrain. When the spectral amplitude of the lower sideband was about one-half that of the original wavetrain, the modulations produced distinct wave packets whose amplitudes were as much as 50% greater than those of the original wavetrains. [Bonmarin & Ramamonjiarisoa (1985) found a similar fast-growing modulation leading to significant amplification of wave amplitudes in their experimental studies of breaking waves.] At this stage three-dimensional, resonant quintets (the "Type II" instability of McLean) grew rapidly, then subsided leaving a two-dimensional wavetrain that exhibited modest modulations and had a frequency that was downshifted from the original sideband growth. Su & Green suggested that the Type I instability triggered the growth of Type II instabilities. They also noted that the coexistence and interactions between these two types of instabilities depended crucially on the tank's width exceeding twice the wavelength of the generated wavetrain. Stiassnie & Shemer (1987) examined the coupled behavior between Type I and Type II instabilities observed in Su's & Green's experiments using their extended Zakharov equation. Their theoretical predictions were qualitatively similar to the measurements of Su & Green; however, Stiassnie & Shemer disagreed with the causality of Type II instabilities by Type I instabilities. Instead, their results suggested that whenever the level of Type I instabilities was substantially greater than that of Type II, the Type II instability was suppressed.

Wu et al (1979) conducted laboratory experiments to investigate the applicability of Hasselmann's stochastic model of wave-wave interactions. They used a wind-wave tank comprising a closed channel, which was 37.7 m long, 2 m high, and 1 m wide; a fan that drew air over a layer of water 1 m deep; and five in situ wave gauges located at 3 m intervals along the 23 m long, glass-walled test section of the tank. They also measured pressure fluctuations in the air channel using crystal pressure transducers placed near each wave gauge. They performed three experiments at wind speeds of 7.1, 8.0, and 8.9 m/s, and obtained continuous time signals from wave gauges and pressure transducers which were amplified, low-pass filtered, and digitized to obtain 40-Hz discrete time signals. They used ten-minute records and partitioned them to form 50 records with which they calculated one-dimensional energy spectra and cross-spectra between the fluctuating pressure and wave heights. These spectra were then ensemble averaged at each gauge site. They used the averaged energy spectra to find the net energy change at each spectral frequency (2–9 Hz) between two gauge sites. The net energy change comprised three processes: energy transferred from the wind to the waves, energy transferred among waves by nonlinear interactions, and energy dissipated by wave breaking and

viscous effects. In order to investigate energy transfer by resonant interactions, it is necessary to isolate each of these three processes, which, as Wu et al note, is extremely difficult to do experimentally. To this end they adopted parametric models for each process. In particular, they replaced the nonlinear wave-wave interactions in Hasselmann's model (14) by a model due to Barnett (1968), in which the measured energy spectra were used as input. Their adopted models for energy dissipation and energy transfer from the wind used the measured energy spectra and cross-spectra as inputs, respectively. They computed theoretical predictions for energy transfer by nonlinear wave-wave interactions using Barnett's model. They computed "experimental" (sic) values for energy transfer by nonlinear wave-wave interactions by subtracting predicted values for energy transfer from the wind and energy dissipation from the measured net energy change. Their comparisons between theoretical and experimental values at four measurement sites showed satisfactory agreement for low and intermediate frequencies, but unsatisfactory agreement at higher frequencies.

Gravity-Capillary and Capillary Wave Experiments

Simmons (1969) derived the governing equations for a degenerate resonant triad of gravity-capillary waves corresponding to second-harmonic resonance, i.e. in Equation (10) $\mathbf{k}_1 = 2\mathbf{k}_0$, $\omega_1 = 2\omega_0$, and $(\mathbf{k}_0, \omega_0)$ correspond to Wilton ripples with $f_0 = 9.8$ Hz. McGoldrick (1970a) elaborated on Simmons' analysis and showed that the permanent-form solution obtained by Wilton (1915) is not expected to occur in a viscous fluid owing to its special choice of initial conditions. McGoldrick (1970b) performed experiments on second-harmonic resonance in which Wilton ripples were generated by a wedge-shaped paddle which was partially immersed in a water surface and oscillated vertically by an electromagnetic servomechanism. The paddle, which had a glass-covered front face, spanned the 61 cm width of a 3 m-long basin. McGoldrick used an in situ wave gauge, capable of detecting wave amplitudes as small as 10^{-3} mm and made measurements at 1 cm intervals away from the paddle. As in previous experiments (McGoldrick et al 1966), he processed the continuous time signals from the wave gauge using a sharply tuned, band-pass filter which enabled him to measure the spectral amplitudes at the wavetrain's fundamental and superharmonic frequencies. McGoldrick used tap water in the experiments and found to his consternation that a surface film was present, requiring him to lower the surface tension value in (22) by about 30% from its clean-surface value. In fact, this lowering of surface tension could not be detected by a du Nouy tensiometer, so McGoldrick used Kelvin's Equation (22) as Rayleigh (1890) had done to measure T. This

film also led to enhanced viscous attenuation of the waves, which were extinguished before they reached the end of the basin. Nevertheless, McGoldrick's experiments clearly showed the strength of second-harmonic resonance; he notes: ". . . the interaction process is so dramatic that it can be seen by eye!" The measured data showed significant growth of the superharmonic amplitude at the expense of the fundamental prior to both waves being extinguished by viscosity. In addition, the relative phase between the two waves remained near its predicted value of $\pi/2$. These striking results occurred in spite of the exceedingly small wave steepnesses ($\varepsilon < 0.05$) used in the experiments. Henderson & Hammack (1987) also performed experiments on Wilton ripples and its second harmonic. When they generated a wavetrain of Wilton ripples, it rapidly transferred a significant portion of its energy to its 19.6-Hz superharmonic, and there was a proliferation of higher-frequency superharmonics in the measured spectra. When they generated a 19.6-Hz wavetrain, it slowly transferred an insignificant portion of its energy to the 9.8-Hz subharmonic; Benjamin-Feir instabilities were dominant. Perlin & Hammack (1991) used remote sensing techniques (described in more detail below) to measure the two-dimensional wavenumber spectrum when a 9.8-Hz wavetrain was generated in a channel. They observed the proliferation of spectral peaks at superharmonic wavenumbers and significant growth of transverse sideband wavenumbers for the 9.8- and 19.6-Hz wavetrains. The absence of sideband growth in frequency spectra indicated that the presence of sideband growth in the wavenumber spectra resulted from rhombus-quartet interactions.

McGoldrick (1972) revisited the second-harmonic resonance for gravity-capillary waves and extended the analysis to the third-harmonic resonance. The analytical features of these two cases were then generalized to fourth-, fifth-, and higher-harmonic resonances. McGoldrick performed experiments on these higher-order internal resonances using apparatus and techniques similar to those of McGoldrick (1970b) except that the water surface was renewed every 20 min by flushing it over a weir so that the surface tension was the clean-surface value. He measured amplitude response curves in the vicinity of the predicted resonant frequencies for third-, fourth-, and sixth-harmonic[4] resonances, and observed strong responses in the vicinity of all of these higher-order resonances. As is common in externally forced systems, the maximum responses occurred at different frequencies (slightly lower) from those predicted by (22). McGoldrick's

[4] McGoldrick's Figure 8 and his corresponding discussion refer to sixth-harmonic resonance throughout; however, the period of 0.144 s labeled in his Figure 8 more closely corresponds to fifth-harmonic resonance.

results also showed that resonance persisted even when there was substantial detuning, so much in fact that the response curves for third- and fourth-harmonic resonance nearly joined. Third-harmonic resonance was excited down to 8.06 Hz while fourth-harmonic resonance was excited up to 7.94 Hz. Perlin & Hammack (1991) explored the small intervening frequency band, and found that third-harmonic resonance occurred for an 8.00-Hz wavetrain. Therefore, internal resonance occurs everywhere within the frequency band between the (discrete) theoretical frequencies of third- and fourth-harmonic resonance. (This behavior is indicated in Figure 1 by the shaded bands about each internal-resonance.) Moreover, both McGoldrick (1972) and Perlin & Hammack (1991) observed that these internal resonances were easily excited by waves with surprisingly small steepnesses. McGoldrick excited sixth-harmonic resonances using a wavetrain with $\varepsilon = 0.15$—although the nonlinear terms responsible for this interaction in the theory are $O(\varepsilon^6)$. The finite width and joining of the internal-resonance response curves and their excitation by exceedingly small wave steepnesses make the stability of wavetrains in the frequency band of 6.4–9.8 Hz to modulations (Hogan 1985) of little practical consequence. These experimental results are testimony to the robustness of internal resonances, but are somewhat disturbing from the perturbative point of view of RIT.

Banerjee & Korpel (1982) generated capillary wavetrains in the frequency range of 30–100 Hz by horizontally oscillating a vertical plate immersed just below the surface of tap water which nearly filled a 30 cm × 30 cm × 5 cm basin. They used an electromagnetic mechanism to drive the paddle, which did not span the basin width. They measured the temporal motion of the water surface with an in situ gauge and its spatial motion by setting the basin on the Fresnel lens of an overhead projector which was modified with a Schlieren system and strobe lamp. This apparatus illuminated the wavefield, forming images with a contrast in light intensities related to the local water depth. The strobe light rendered the images stationary so that photographs could be made. Banerjee & Korpel found that subharmonic wavetrains occurred in all of their experiments when the paddle stroke exceeded a threshold value. These subharmonic waves formed a standing-wave pattern which was readily observed at the wavemaker and to its side. They attributed these results to a resonant triad between the generated wavetrain and two oblique, subharmonic wavetrains. Henderson & Hammack (1987) performed similar experiments, but did not observe the subharmonic behavior reported by Banerjee & Korpel. Based on Hogan's (1984) reinterpretation of Banerjee's & Korpel's data, which indicated that strongly nonlinear waves were being generated, and their own experiments, Henderson & Hammack (1987) cited

a list of circumstantial evidence indicating that subharmonic cross waves—which are a strongly nonlinear, trapped wave phenomenon and outside the purview of weakly nonlinear RIT—were generated by Banerjee & Korpel.

Banerjee et al (1983) used the experimental apparatus described above to examine the weakly nonlinear phenomenon of focusing, which occurs in (17) and is discussed in the context of water waves by Ablowitz & Segur (1979) and Peregrine (1983). According to (17), a localized packet of short-crested waves with frequencies greater than that of Wilton ripples will evolve a singularity in finite time as a consequence of focusing. The phenomenon of focusing is easily understood using the nonlinear dispersion relations given by Wilton (1915), i.e.

$$c(k \approx k_0; \varepsilon) = 3\left(\frac{gT}{2\varrho}\right)^{1/4}\left(1 \mp \frac{1}{4}\varepsilon\right), \tag{23}$$

and using the analysis of Pierson & Fife (1961) for wavetrains with wavenumbers near $k = k_0$. In (23) the upper $(-)$ sign is chosen for waves with $k > k_0$ and the lower $(+)$ sign is chosen for waves with $k < k_0$. When a short-crested wavetrain is generated with $k > k_0$, large-amplitude regions of crests propagate more slowly than low-amplitude regions so that the crests turn on themselves, i.e. they focus when $\partial c/\partial \varepsilon < 0$. When a short-crested wavetrain is generated with $k < k_0$, the wave crests bend in opposite directions, i.e. they defocus when $\partial c/\partial \varepsilon > 0$. Banerjee et al (1983) used a wave paddle with a length of 3 cm to generate localized packets of short-crested wavetrains with frequencies of 20, 30, and 50 Hz; focusing was expected for all of these wavetrains. They observed focusing for the 30- and 50-Hz wavetrains, but not for the 20-Hz wavetrain. They gave no explanation for the absence of focusing by the 20-Hz wavetrain.

Perlin & Hammack (1991) performed experiments on gravity-capillary and capillary wavetrains with frequencies of 8.0–25.0 Hz and moderate steepnesses ($\varepsilon < 0.3$). They conducted experiments in a wave channel measuring 91 cm $\times$ 30.5 cm with a water depth of 4.9 cm. They generated wavetrains using a wedge-shaped paddle which spanned the channel width and was oscillated vertically in the water surface by an electromagnetic servomechanism. They cleaned all of the materials contacting the water with ethyl alcohol before each experiment and used doubly distilled water which was filtered of organic material, minerals, and particles with nominal sizes greater than 0.2 μm. They measured water surface motion at different positions along the channel using an in situ wave gauge. Continuous time signals were band-pass filtered, amplified, and sampled at 250 Hz to obtain discrete time signals. They used these data to compute amplitude-fre-

quency spectra with a frequency resolution of 0.015 Hz. In addition, they measured two-dimensional wavenumber spectra of wavefields using a high-speed imaging system with an imager looking down on the water surface from above the channel. The imager comprised a 128×128 pixel array that measured discrete-space gray-levels in a 22 cm $\times$ 22 cm surface area, which began 23 cm from the wavemaker; the wavenumber resolution was 0.284 rad/cm. An image calibration showed that the correlation coefficient between these gray levels and measurements of a nearby in situ wave gauge was 0.89. All of the frequency and wavenumber spectra for wavetrains in the frequency range 9.8–19.6 Hz, in which resonant quartets are the first to occur, showed the following results: (*a*) Frequency spectra showed distinct spectral peaks at frequencies of the generated wavetrain and its superharmonics with no indication of sideband growth. (*b*) Wavenumber spectra showed spectral amplitudes spreading outward from the peak of the generated wavetrain in a circular arc with a radius equal to the magnitude of the generated wavetrain's wavevector. In other words, rhombus-quartet sideband instabilities were dominant. (The latter result is apparent in Figure 3, which is taken from Perlin et al (1990) and is discussed below.) Perlin & Hammack (1991) compared their measurements to predictions of the NLS Equations (19) and (20) for longitudinal and transverse sideband growth, respectively. There was some evidence of longitudinal sideband growth in the wavenumber spectra, but much less than predicted by (19). On the other hand, there was much more growth of transverse sideband amplitudes (at the frequency of the generated wavetrain) than predicted by (20). This dominance of sideband rhombus-quartet instabilities was not predicted by the numerical calculations of Zhang & Melville (1987) using the unapproximated (Euler) equations. Perlin & Hammack also found that sideband rhombus-quartet instabilities remained dominant for wavetrains with $f > 19.6$ Hz where resonant triads are possible—when the phenomenon of selective amplification (Henderson & Hammack 1987, Perlin et al 1990) does not occur.

Henderson & Hammack (1987) reported experiments on the stability of capillary wavetrains with frequencies of 22–46 Hz where resonant triad interactions are expected to occur. They used the experimental facilities and procedures described in Perlin & Hammack (1991). Their experiments were designed specifically to test the stability of wavetrains for which resonant triads are possible, as predicted by Simmons (1969) for an elementary resonant triad of capillary waves. Simmons showed that a generated wavetrain, say $(\mathbf{k}_1, \omega_1)$, can form resonant triads with two waves (summed) from a continuum of waves in a lower-frequency (closed) band B_l and with two waves (differenced) from a higher-frequency (open-ended) band B_h. Simmons also showed that waves in B_h could not amplify when their

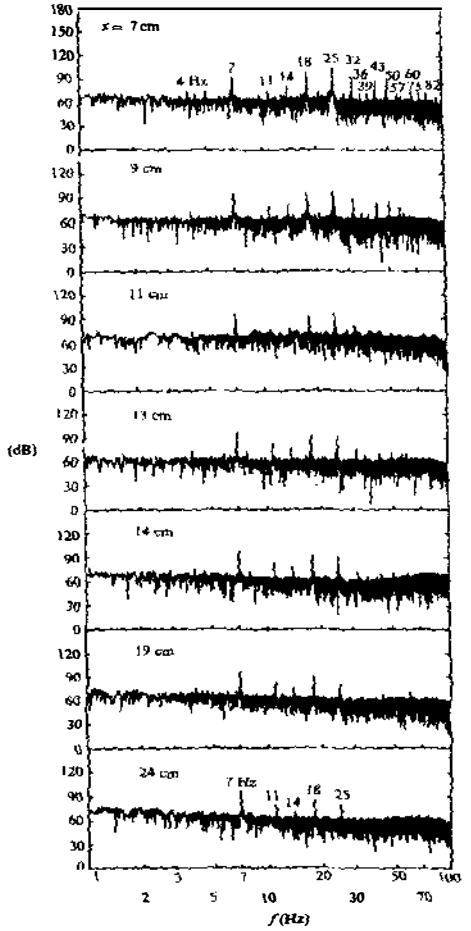

Figure 2 Spatial evolution of the amplitude-frequency spectrum for a 25-Hz wavetrain in the presence of a 57-Hz background wavetrain; $h = 5$ cm, $T = 73$ dyn/cm (from Perlin et al 1990; courtesy of Cambridge University Press).

amplitudes were infinitesimal relative to that of the generated wavetrain. [This result is generally true for resonant triads according to a theorem by Hasselmann (1967b).] Waves in B_l can amplify; however, since the interaction coefficients of (13) vary smoothly across B_l, Simmons conjectured that selective amplification is unlikely. Instead, all of the background waves in B_l are expected to amplify and destabilize the generated wavetrain. Henderson's & Hammack's experiments showed that wavetrains with $f > 19.6$ Hz were unstable to background waves with frequencies in B_l; however, in most experiments a single triad with two waves from B_l was selectively amplified. In some experiments, the spectral amplitude(s) of the wave(s) in B_l grew, decayed, and grew again during propagation down the channel, i.e. energy cycled, as the exact solutions of the three-wave equations suggest. Henderson & Hammack did not measure wavenumber spectra in their experiments; however, this cyclic behavior, which cannot occur in nonresonant interactions, led them to conjecture that the waves in B_l formed a resonant triad with the generated wavetrain. In their experiments the selected triad varied with the frequency of the generated wavetrain. However, the same triad amplified repeatably, regardless of the generated wavetrain's amplitude, which was increased from its viscous threshold value until subharmonic cross waves evolved at the wavemaker paddle. They gave no explanation for either the presence of selective amplification in some experiments or its absence in others.

A surprising and serendipitous answer to the riddle of selective amplification described above was found by Perlin et al (1990). When a new computer system was installed in the laboratory, Perlin et al conducted the experiments of Henderson & Hammack (1987), and found *no* triads selectively amplified. When they repeated the experiments with the older computer system, selective amplification returned. They traced the different results to the computers' analog output systems, which provided command signals to the wavemaker. Both devices were comparable in specification; however, the inadvertent noise level at the electrical power frequency of 60 Hz was about 1/5 lower in the newer device. This small difference, which was represented by signal-to-noise ratios of about 100 in the older device and 200 in the newer device, was sufficient to alter radically the outcome of an experiment. Perlin et al (1990) conjectured the following explanation of and algorithm for predicting selective amplification of two wavetrains in B_l by a wavetrain f_1 of moderate amplitude and an infinitesimal background wavetrain f_0 in B_h. First, both f_1 and f_0 become directionally unstable by sideband rhombus-quartet instabilities described by Perlin & Hammack (1991). This instability is crucial since f_1 and f_0 are initially collinear and generally cannot satisfy (10a) with any other wavetrain. The directional instability allows wavetrains to amplify with the

proper wavevector configurations to satisfy (10a). Thereby the generated wavetrains form a resonant triad with the difference wavetrain (f_0-f_1). The difference wavetrain cannot amplify in accordance with Hasselmann's (1967b) theorem; however, Perlin et al used numerical calculations of the three-wave equations to show that (f_0-f_1) does exchange energy with f_0. Second, (f_0-f_1) becomes directionally unstable and a new resonant triad forms with frequencies $(f_1, f_0-f_1, 2f_1-f_0)$. Again, the new difference wavetrain cannot amplify but it does exchange energy with the previous difference wavetrain. This process continues until a difference wavetrain with a frequency in B_l, say f_2, is excited and becomes directionally unstable; since f_2 is in B_l, it can and does amplify. Thereby a resonant triad with frequencies (f_1, f_2, f_1-f_2) is seeded by f_0 and is selectively amplified. This algorithm can be continued to determine if more than one triad with two waves in B_l can be selectively amplified. The algorithm comprises exceedingly weak nonlinear interactions that are normally ignored; yet, when they occurred, they determined the outcome of an experiment. Perlin et al used this algorithm and correctly predicted the presence and absence of selective amplification in all of the experiments in Henderson & Hammack (1987). Since the 60-Hz noise level of the newer computer system was below the threshold to cause selective amplification, Perlin et al (1990) added artificial noise at discrete frequencies in B_h and tested their algorithm further. Results from one of their experiments is shown in Figure 2, which presents amplitude-frequency spectra computed from the discrete time signals (sampled at 250 Hz) of a wave gauge at various distances (x) from the wavemaker. They programmed the wavemaker to generate a 25-Hz wavetrain with steepness $\varepsilon \approx 0.20$ and a 57-Hz wavetrain with steepness $\varepsilon \approx 0.04$. According to their selection algorithm, two triads with waves in B_l, which has the range of about 5.0–20.0 Hz, were possible: The first triad to occur comprised wavetrains with frequencies of 25, 7, and 18 Hz; the second triad comprised wavetrains with frequencies of 25, 11, and 14 Hz. At the first station of measurement in Figure 2 ($x = 7$ cm), which is seven wavelengths of the 25-Hz wavetrain from the wavemaker, superharmonics and sum-and-difference wavetrains proliferate; the 57-Hz wavetrain is barely discernible. At the last measurement station ($x = 24$ cm), five distinct wavetrains dominate, and they correspond to those expected in the two, coupled resonant triads. The spectral amplitudes of the 7- and 18-Hz wavetrain at $x = 24$ cm are larger than those of the 25-Hz wavetrain. The spectral amplitudes of the 25-Hz wavetrain gradually diminish during propagation while those of the 7-Hz wavetrain, which is already large by $x = 7$ cm, remain about constant. The spectral amplitudes of the 18-Hz wavetrain, which is already large by $x = 7$ cm, decrease slightly, then increase slightly, and then decrease again during propagation. The spectral

amplitudes of the 11- and 14-Hz wavetrains grow, diminish, disappear, reemerge, grow, and diminish again during propagation. This behavior strongly suggests that two, coupled triads are evolving in the wave channel. Perlin et al also measured two-dimensional wavenumber spectra using the apparatus described in Perlin & Hammack (1991). The result for one image is shown in Figure 3, which shows ten equally spaced contour levels of the spectral amplitudes in the positive quadrant of wavenumber space. The wavenumber axes (l, m) are rotated so that the wavevector of the 25-Hz wavetrain generated by the wavemaker bisects this quadrant. The circles drawn in Figure 3 correspond to the isotropic dispersion relation (22) at frequencies of 25, 18, 14, 11, and 7 Hz. Wave energy is concentrated in arcs at wavenumbers corresponding to the aforementioned wave frequencies; hence, they are free waves resulting from resonant interactions. Moreover, the directional spread of the wave energy about these circular arcs is a manifestation of sideband rhombus-quartet instabilities—necessary in order for the wavetrains to have the proper wavevector configurations satisfying (10a).

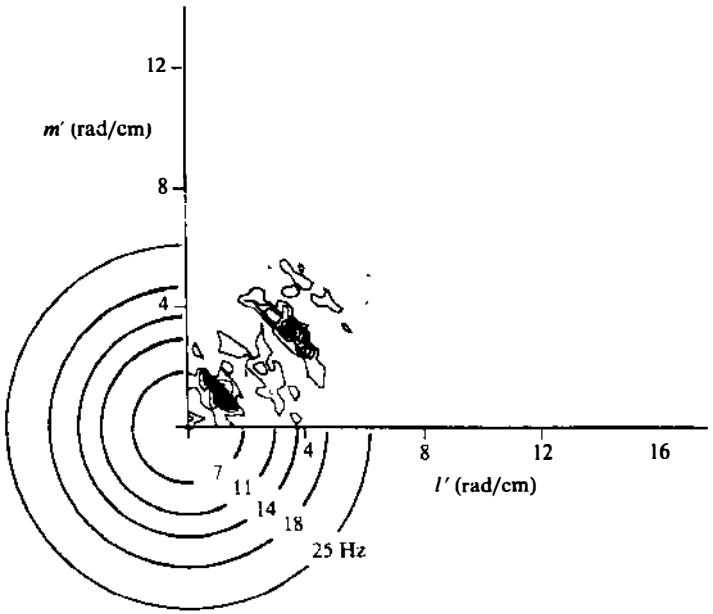

Figure 3 Contour map of amplitude-wavevector spectrum for a 25-Hz wavetrain in the presence of a 57-Hz background wavetrain; $h = 5$ cm, $T = 73$ dyn/cm (from Perlin et al 1990; courtesy of Cambridge University Press).

The sensitivity of triadic resonances among capillary wavetrains to discrete components in ubiquitous background noise led Perlin et al (1990) to an experimental investigation in which they added artificial "white" noise at the wavemaker to the dominant wavetrain and, in some experiments, a discrete noise component which seeded selective amplification. They characterized the broad-spectrum background noise by a signal-to-noise ratio (SNR) defined as

$$\text{SNR} = \frac{\text{rms of wavetrain signal}}{\text{rms of white noise signal}},$$

in which rms is the root-mean-square of deviations in the command signal voltages from their mean value. (The relationship between voltage and stroke of the wavemaker was nearly linear.) They found that selective amplification was reduced when the broad-spectrum background noise was amplified; it disappeared completely when the SNR of the discrete noise component was about 1/10. They then examined the effect of (only) broad-spectrum random noise on the evolution of a dominant wavetrain by conducting experiments in the following manner. First, they obtained 16 discrete time series of wave gauge data and computed frequency spectra for the natural background noise in the tank when the wavemaker was powered, but not moving. These 16 frequency spectra were ensemble averaged to obtain a representative spectrum for the natural background noise, $\langle \mathfrak{B} \rangle$, in the tank. Then they conducted 16 experiments using white-noise command signals to the wavemaker. Wave gauge data were obtained and analyzed for each experiment and an ensemble-averaged frequency spectrum for the random waves in the presence of the tank's natural background noise, $\langle \mathfrak{R}+\mathfrak{B} \rangle$, was found. Using only a 25-Hz wavetrain, an additional 16 experiments were performed to find an ensemble-averaged frequency spectrum for the dominant wavetrain in the presence of the tank's natural background noise, $\langle \mathfrak{T}+\mathfrak{B} \rangle$. Then they added the dominant-wavetrain signal (SNR = 10) to the 16 command signals of white noise and conducted 16 more experiments to find an ensemble-averaged frequency spectrum for the dominant wavetrain with random waves and the tank's background noise, $\langle \mathfrak{T}+\mathfrak{R}+\mathfrak{B} \rangle$. They combined these four ensembled-averaged spectra linearly to obtain the average frequency spectrum for the random waves alone, i.e. $\langle \mathfrak{R} \rangle = \langle \mathfrak{R}+\mathfrak{B} \rangle - \langle \mathfrak{B} \rangle$ and the dominant wavetrain alone, i.e. $\langle \mathfrak{T} \rangle = \langle \mathfrak{T}+\mathfrak{B} \rangle - \langle \mathfrak{B} \rangle$. To display the effects of nonlinear interactions they calculated

$$\langle \mathfrak{N} \rangle := \langle \mathfrak{T}+\mathfrak{R}+\mathfrak{B} \rangle - \langle \mathfrak{T} \rangle - \langle \mathfrak{R} \rangle - \langle \mathfrak{B} \rangle; \tag{24}$$

hence, $\langle \mathfrak{N} \rangle$ is null if nonlinear interactions are insignificant. (They tacitly

assumed that the natural background noise in the tank was sufficiently small to interact linearly with the random and dominant wavetrains.) They performed this series of experiments at three gauge sites downstream of the wavemaker. Their main results are presented in Figure 4 where the ensemble-averaged spectra $\langle \mathfrak{N} \rangle$ are shown at three downstream measurement stations. Note that $\langle \mathfrak{N} \rangle$ is not null, indicating that significant non-

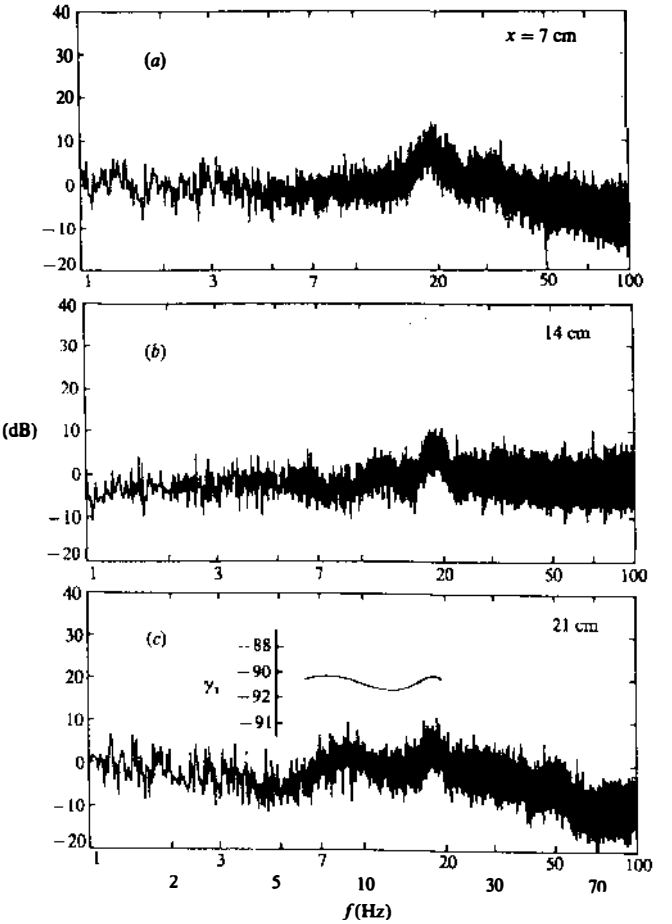

Figure 4 Evolution of the ensemble-averaged spectrum $\langle \mathfrak{N} \rangle$, which shows the effects of nonlinear wave-wave interactions, down the channel; $h = 5$ cm, $T = 73$ dyn/cm. Inset shows the theoretical interaction coefficients γ_1 for triadic interactions across B_1 (from Perlin et al 1990; courtesy of Cambridge University Press).

linear interactions occurred. At $x = 7$ cm, spectral amplitudes between 16 and 22 Hz increased with a maximum amplification at 19 Hz. Note that this frequency band is in and near the low-frequency continuum B_l (5.0–20.0 Hz) of the 25-Hz wavetrain. Spectral amplitudes in the high-frequency continuum B_h (≥ 30.0 Hz) decreased. At $x = 14$ cm spectral amplitudes between 1 and 7 Hz decreased while those between 7 and 22 Hz increased in a bimodal manner with maxima near 12 and 19 Hz and a minimum near 15 Hz. Beyond 22 Hz, spectral amplitudes at $x = 14$ cm show no amplification or attenuation; hence, the waves in B_h have actually gained energy while propagating from $x = 7$ cm. At $x = 21$ cm spectral amplitudes from 1–6 Hz remained lowered while amplitudes in B_h decreased again. The spectral amplitudes in B_l remain amplified with the bimodal distribution observed at the previous measurement station. This spectral distribution is similar to the form of the dynamical interaction coefficient γ_l in (13) over B_l for the 25-Hz wavetrain, which is shown superposed in Figure 4. Perlin et al concluded that, when the background noise spectrum is broad-banded, all of the wavetrains in the low-frequency continuum are amplified by a dominant wavetrain in accordance with predictions of RIT for elementary resonant triads.

CONCLUDING REMARKS

We have reviewed a variety of theoretical investigations (RIT) that were founded on Phillips' (1960) view that resonant wave-wave interactions play a special role. These theoretical investigations branched in two directions. Deterministic investigations included studies of wavefields comprised of resonant interactions among a single triad or a single quartet of waves, a small number of coupled triads or quartets, or a narrow spectrum of waves. Stochastic investigations included studies of wavefields comprised of resonant interactions among either a broad or a narrow spectrum of waves. We have also reviewed a variety of experimental investigations (RIE) that enabled some aspects of RIT to be tested. These experimental investigations branched in four directions. There are numerous experimental investigations that studied the validity of Kelvin's linear dispersion and the stability of a single wavetrain to artificial and naturally occurring background perturbations. We have found only two experimental investigations that have studied the interactions among more than one wavetrain of comparable (initial) amplitudes and only one experimental investigation that addressed the relative roles of nonlinearity and randomness for a broad spectrum of waves.

Many meticulous laboratory experiments showed that Kelvin's dispersion relation for infinitesimal waves (22), which is crucial to all appli-

cations of resonant interaction theory, is accurate over a wide range of frequencies, even for wavetrains with moderate steepnesses. Good quantitative agreement between theoretical and experimental investigations of wavetrain stability was found for the celebrated Benjamin-Feir (B-F) instability, which is a degenerate resonant four-wave interaction between two wavetrains (each counted twice) that are collinear or nearly collinear and have nearly the same frequencies and wavevector magnitudes. Good qualitative agreement persisted for wavetrains with near-breaking steepnesses in experiments that used narrow (relative to wavelength) channels, which inhibited oblique B-F instabilities. Results differed dramatically between gravity and gravity-capillary wavetrains in experiments that used wide channels, which allowed for the possibility of oblique instabilities. For gravity waves with initially moderate steepnesses, evolution comprised a sequence of two- and three-dimensional instabilities, which included the collinear B-F instability. However, these instabilities occurred too rapidly for a straightforward application of RIT, which supposes a rank ordering of disparate time scales for resonant triads, quartets, quintets, etc. For gravity-capillary and capillary wavetrains with initially moderate steepnesses, evolution was dominated by degenerate rhombus-quartet instabilities; this dominance is not predicted by existing RIT. In the absence of the phenomenon of selective amplification, rhombus-quartet instabilities were also dominant for capillary wavetrains, even though resonant-triad interactions are possible.

Selective amplification is an experimentally observed phenomenon in which a discrete background wave with exceedingly small steepness seeds the destabilization of a capillary wavetrain by one or more (coupled) resonant triads. Seeding appears to occur through a sequence of weak, dynamically nonresonant interactions that are normally neglected; yet, when they occur, they determine the outcome of an experiment. Whether selection occurs depends on the nature of the ubiquitous high-frequency background noise—present in any water-wave system. If the high-frequency spectrum of background noise is narrow-banded so that it contains a discrete component, selection occurs. If the spectrum is broad-banded, selection does not occur. In the latter case, experiments suggest that the entire continuum of dynamically possible low-frequency triads evolve according to RIT for single resonant triads.

The important role of degenerate resonances was also shown by the internal resonances known as Wilton ripples. These resonances, which were observed to $O(\varepsilon^6)$, are excited by wavetrains with exceedingly small steepnesses and with significant frequency detuning. In fact, these internal resonances effectively fill the band of modulationally stable wavetrains (6.4–9.8 Hz). Internal resonant interactions, like the sequence of inter-

actions that lead to selective amplification, evolve quickly so that the rank ordering of evolution time scales supposed by RIT is violated.

Experimental investigations have focused on the degenerate resonances that play an especially important role for studying the stability of a single wavetrain, almost to the exclusion of studies on nondegenerate resonances, i.e. resonant interactions among wavetrains which satisfy (10) and (11) with arbitrary frequencies and wavevector configurations. The absence of controlled experiments to test RIT in this general, deterministic setting is striking; in fact, we found only one controlled experiment in which two different wavetrains were generated by two wavemakers and their interaction studied—and this was the first experiment reported in the companion papers by Longuet-Higgins & Smith (1966) and McGoldrick et al (1966) which established the special role of resonant interactions. The absence of controlled experiments to test RIT in its general stochastic settings is even more striking. We found only one experimental investigation that attempted to establish the validity of stochastic models that use the random phase approximation, which requires randomness to dominate nonlinear wave-wave interactions. That experiment used wind to generate nearly collinear wavetrains in a laboratory channel. While wind generation resembles the oceanic application of the stochastic models, it does not allow definitive conclusions about the relative roles of nonlinearity and randomness because of poorly understood contributions from wind and wave-breaking processes.

Phillips (1981a) noted that perhaps the simple ideas of resonant interaction theory have reached their natural limits and that further progress would depend on new mathematics, new physics, and new intuition. Perhaps this new intuition and new physics may be found in the richness of behavior observed in resonant interaction experiments.

ACKNOWLEDGMENTS

JLH is grateful for financial support by the Office of Naval Research under contract N00014-89-J-1335 and the Army Research Office under contract DAAL03-89-K-0150.

Literature Cited

Ablowitz, M. J., Haberman, R. 1975a. Nonlinear evolution equations—two and three dimensions. *Phys. Rev. Lett.* 35: 1185–88

Ablowitz, M. J., Haberman, R. 1975b. Resonantly coupled nonlinear evolution equations. *J. Math. Phys.* 16: 2301–5

Ablowitz, M. J., Kaup, D. J., Newell, A. C., Segur, H. 1974. The inverse scattering transform-Fourier analysis for nonlinear problems. *Stud. Appl. Math.* 53: 249–315

Ablowitz, M. J., Segur, H. 1979. On the evolution of packets of water waves. *J. Fluid Mech.* 92: 691–715

Ablowitz, M. J., Segur, H. 1981. *Solitons and the Inverse Scattering Transform.* Philadelphia: S.I.A.M.

Adamson, A. W. 1990. *Physical Chemistry of Surfaces.* New York: Wiley. 5th ed.

Alber, I. E. 1978. The effects of randomness on the stability of two-dimensional surface wavetrains. *Proc. R. Soc. London Ser. A* 363: 525–46

Ball, F. K. 1964. Energy transfer between external and internal gravity waves. *J. Fluid Mech.* 19: 465–78

Banerjee, P. P., Korpel, A. 1982. Subharmonic generation by resonant three-wave interaction of deep-water capillary waves. *Phys. Fluids* 25: 1938–43

Banerjee, P. P., Korpel, A., Lonngren, K. E. 1983. Self-refraction of nonlinear capillary-gravity waves. *Phys. Fluids* 26: 2393–98

Barnett, T. P. 1968. On the generation, dissipation, and prediction of ocean wind waves. *J. Geophys. Res.* 73: 513–29

Barrick, D. E. 1986. The role of the gravity-wave dispersion relation in HF radar measurements of the sea surface. *IEEE J. Ocean. Eng.* 11: 286–92

Benjamin, T. B. 1967. Instability of periodic wavetrains in nonlinear dispersive systems. *Proc. R. Soc. London Ser. A* 299: 59–75

Benjamin, T. B., Feir, J. E. 1967. The disintegration of wavetrains on deep water. *J. Fluid Mech.* 27: 417–30

Benney, D. J. 1962. Non-linear gravity wave interactions. *J. Fluid Mech.* 14: 577–84

Benney, D. J., Newell, A. C. 1967. The propagation of nonlinear wave envelopes. *J. Math. Phys.* 46: 133–39

Benney, D. J., Newell, A. C. 1969. Random wave closures. *Stud. Appl. Math.* 48: 29–53

Benney, D. J., Roskes, G. J. 1969. Wave instabilities. *Stud. Appl. Math.* 48: 377–85

Benney, D. J., Saffman, P. G. 1966. Nonlinear interactions of random waves in a dispersive medium. *Proc. R. Soc. London Ser. A* 289: 301–20

Bonmarin, P., Ramamonjiarisoa, A. 1985. Deformation to breaking of deep water gravity waves. *Exp. Fluids* 3: 11–16

Boyd, T. J. M., Turner, J. G. 1978. Three- and four-wave interactions in plasmas. *J. Math. Phys.* 19: 1403–13

Bretherton, F. P. 1964. Resonant interactions between waves. The case of discrete oscillations. *J. Fluid Mech.* 20: 457–79

Cini, R., Lombardini, P. P. 1978. Damping effect of monolayers on surface wave motion in a liquid. *J. Colloid Interface Sci.* 65: 387–89

Craik, A. D. D. 1985. *Wave Interactions and Fluid Flows.* Cambridge: Cambridge Univ. Press

Craik, A. D. D. 1986. Exact solutions of non-conservative equations for three-wave and second-harmonic resonance. *Proc. R. Soc. London Ser. A* 406: 1–12

Craik, A. D. D., Moroz, I. M. 1988. Temporal evolution of interacting waves in non-conservative systems: some exact solutions. *Wave Motion* 10: 443–52

Crawford, D. R., Saffman, P. G., Yuen, H. C. 1980. Evolution of a random inhomogeneous field of nonlinear deep-water gravity waves. *Wave Motion* 2: 1–16

Crawford, D. R., Lake, B. M., Saffman, P. G., Yuen, H. C. 1981a. Stability of weakly nonlinear deep-water waves in two and three dimensions. *J. Fluid Mech.* 105: 177–91

Crawford, D. R., Lake, B. M., Saffman, P. G., Yuen, H. C. 1981b. Effects of nonlinearity and spectral bandwidth on the dispersion relation and component phase speeds of surface gravity waves. *J. Fluid Mech.* 112: 1–32

Davey, A., Stewartson, K. 1974. On three-dimensional packets of surface waves. *Proc. R. Soc. London Ser. A* 338: 101–10

Davidson, R. C. 1972. *Methods in Nonlinear Plasma Theory.* New York: Academic

Davies, J. T., Vose, R. W. 1965. On the damping of capillary waves by surface films. *Proc. R. Soc. London Ser. A* 286: 218–34

Djordjevic, V. D., Redekopp, L. G. 1977. On two-dimensional packets of capillary-gravity waves. *J. Fluid Mech.* 79: 703–14

Dobroklonskii, S. V. 1955. The damping of capillary-gravity waves on the surface of clean water. *Tr. M.G.I. Akad. Nauk SSSR* 6: 43–57 (In Russian)

Dungey, J. C., Hui, W. H. 1979. Nonlinear energy transfer in a narrow gravity-wave spectrum. *Proc. R. Soc. London Ser. A* 368: 239–65

Dysthe, K. B. 1979. Note on a modification to the nonlinear Schroedinger equation for application to deep water waves. *Proc. R. Soc. London Ser. A* 369: 105–14

Feir, J. E. 1967. Discussion: some results from wave pulse experiments. *Proc. R. Soc. London Ser. A* 299: 54–58

Fox, M. J. H. 1976. On the nonlinear transfer of energy in the peak of a gravity-wave spectrum. II. *Proc. R. Soc. London Ser. A* 348: 467–83

Freundlich, H. 1922. *Colloid and Capillary Chemistry.* Transl. H. S. Hatfield. New York: Dutton

Gotwols, B. L., Irani, G. B. 1980. Optical determination of the phase velocity of short gravity waves. *J. Geophys. Res.* 85: 3964–70

Hara, T., Mei, C. C. 1991. Frequency downshift in narrowbanded surface waves under the influence of wind. *J. Fluid Mech.* 230: 429–77

Harrison, W. J. 1909. The influence of viscosity and capillarity on waves of finite amplitude. *Proc. London Math. Soc.* 7: 107–21

Hasimoto, H., Ono, H. 1972. Nonlinear modulation of gravity waves. *J. Phys. Soc. Jpn.* 33: 805–11

Hasselmann, K. 1962. On the non-linear energy transfer in a gravity-wave spectrum. Part 1. General theory. *J. Fluid Mech.* 12: 481–500

Hasselmann, K. 1963a. On the non-linear energy transfer in a gravity-wave spectrum. Part 2. Conservation theorems; wave-particle analogy; irreversibility. *J. Fluid Mech.* 15: 273–81

Hasselmann, K. 1963b. On the non-linear energy transfer in a gravity-wave spectrum. Part 3. Evaluation of the energy flux and swell-sea interaction for a Neumann spectrum. *J. Fluid Mech.* 15: 385–98

Hasselmann, K. 1966. Feynman diagrams and interaction rules of wave-wave scattering processes. *Rev. Geophys.* 4: 1–32

Hasselmann, K. 1967a. Nonlinear interactions treated by the methods of theoretical physics (with application to the generation of waves by wind). *Proc. R. Soc. London Ser. A* 299: 77–100

Hasselmann, K. 1967b. A criterion for nonlinear wave stability. *J. Fluid Mech.* 30: 737–39

Hasselmann, K., Barnett, T. P., Bouws, E., Carlson, H., Cartwright, D. E., et al. 1973. Measurements of wind-wave growth and swell decay during the Joint North Sea Wave Project (JONSWAP). *Dtsch. Hydrogr. Z.* A8, No. 12. 95 pp.

Hasselmann, S., Hasselmann, K. 1985. Computations and parametcrizations of thc nonlinear energy transfer in a gravity-wave spectrum. Part I: A new method for efficient computations of the exact nonlinear transfer integral. *J. Phys. Oceanogr.* 15: 1369–77

Hasselmann, S., Hasselmann, K., Allender, J. H., Barnett, T. P. 1985. Computations and parameterizations of the nonlinear energy transfer in a gravity-wave spectrum. Part II: Parameterizations of the nonlinear energy transfer for application in wave models. *J. Phys. Oceanogr.* 15: 1378–91

Hatori, M., Toba, Y. 1983. Transition of mechanically generated regular waves to wind waves under the action of wind. *J. Fluid Mech.* 130: 397–409

Hayes, W. D. 1973. Group velocity and nonlinear dispersive wave propagation. *Proc. R. Soc. London Ser. A* 332: 199–221

Henderson, D. M., Hammack, J. L. 1987. Experiments on ripple instabilities. Part 1. Resonant triads. *J. Fluid Mech.* 184: 15–41

Henderson, D. M., Lee, R. C. 1986. Laboratory generation and propagation of ripples. *Phys. Fluids* 29: 619–24

Hogan, S. J. 1984. Subharmonic generation of deep-water capillary waves. *Phys. Fluids* 27: 42–45

Hogan, S. J. 1985. The fourth-order evolution equation for deep-water gravity-capillary waves. *Proc. R. Soc. London Ser. A* 402: 359–72

Hogan, S. J. 1986. The potential form of the fourth-order evolution equation for deep-water gravity-capillary waves. *Phys. Fluids* 29: 3479–80

Holliday, D. 1977. On nonlinear interactions in a spectrum of inviscid gravity-capillary surface waves. *J. Fluid Mech.* 83: 737–49

Huang, N. E. 1981. Comment on "Modulation characteristics of sea surface waves" by A. Ramamonjiarisoa and E. Mollo-Christensen. *J. Geophys. Res.* 86: 2073–75

Huang, N. E., Tung, C.-C. 1977. The influence of the directional energy distribution on the nonlinear dispersion relation in a random gravity wave field. *J. Phys. Oceanogr.* 7: 403–14

Janssen, P. A. E. M. 1983a. On a fourth-order envelope equation for deep-water waves. *J. Fluid Mech.* 126: 1–11

Janssen, P. A. E. M. 1983b. Long-time behaviour of a random inhomogeneous field of weakly nonlinear surface gravity waves. *J. Fluid Mech.* 133: 113–32

Kaup, D. J. 1981. The solution of the general initial value problem for the full three dimensional three-wave resonant interaction. *Physica* 3D: 374–95

Kelvin, Lord (Thompson, W.) 1871. Part IV. (Letter to Professor Tait, of date August 23, 1871.) and Part V. Waves under motive power of gravity and cohesion jointly, without wind. *Phil. Mag.* XLII: 370–77

Komen, G. J. 1980. Spatial correlations in wind-generated water waves. *J. Geophys. Res.* 85: 3311–14

Lake, B. M., Yuen, H. C. 1977. A note on some nonlinear water-wave experiments and the comparison of data with theory. *J. Fluid Mech.* 83: 75–81

Lake, B. M., Yuen, H. C., Rungaldier, H., Ferguson, W. E. 1977. Nonlinear deep-water waves: theory and experiment. Part 2. Evolution of a continuous wave train. *J. Fluid Mech.* 83: 49–74

LeBlond, P. H., Mysak, L. A. 1978. *Waves in the Ocean.* New York: Elsevier Oceanogr. Ser. Vol. 20

Levich, V. G. 1962. *Physicochemical Hydrodynamics*. Transl. Scripta Technica, Inc. Englewood Cliffs: Prentice-Hall (From Russian)

Lighthill, M. J. 1965. Contributions to the theory of waves in non-linear dispersive systems. *J. Inst. Math. Its Appl.* 1: 269–306

Lo, E., Mei, C. C. 1985. A numerical study of water-wave modulation based on a higher-order nonlinear Schroedinger equation. *J. Fluid Mech.* 150: 395–416

Lo, E. Y., Mei, C. C. 1987. Slow evolution of nonlinear deep water waves in two horizontal directions: a numerical study. *Wave Motion* 9: 245–59

Longuet-Higgins, M. S. 1962. Resonant interactions between two trains of gravity waves. *J. Fluid Mech.* 12: 321–32

Longuet-Higgins, M. S. 1976. On the nonlinear transfer of energy in the peak of a gravity-wave spectrum: a simplified model. *Proc. R. Soc. London Ser. A* 347: 311–28

Longuet-Higgins, M. S. 1977. Some effects of finite steepness on the generation of waves by wind. In *A Voyage of Discovery*, ed. M. Angel, pp. 393–403. New York: Pergamon

Longuet-Higgins, M. S. 1978a. The instabilities of gravity waves of finite amplitude in deep water I. Superharmonics. *Proc. R. Soc. London Ser. A* 360: 471–88

Longuet-Higgins, M. S. 1978b. The instabilities of gravity waves of finite amplitude in deep water II. Subharmonics. *Proc. R. Soc. London Ser. A* 360: 489–505

Longuet-Higgins, M. S., Phillips, O. M. 1962. Phase velocity effects in tertiary wave interactions. *J. Fluid Mech.* 12: 333–36

Longuet-Higgins, M. S., Smith, N. D. 1966. An experiment on third-order resonant wave interactions. *J. Fluid Mech.* 25: 417–35

Martin, D. U., Yuen, H. C. 1980. Quasi-recurring energy leakage in the two-space-dimensional nonlinear Schroedinger equation. *Phys. Fluids* 23: 881–83

Masuda, A. 1981. Nonlinear energy transfer between wind waves. *J. Phys. Oceanogr.* 10: 2082–93

Masuda, A. 1986. Nonlinear energy transfer between random gravity waves. Some computational results and their interpretation. In *Wave Dynamics and Radio Probing of the Ocean Surface*, ed. O. M. Phillips, K. Hasselmann, pp. 41–57. New York: Plenum

McGoldrick, L. F. 1965. Resonant interactions among capillary-gravity waves. *J. Fluid Mech.* 21: 305–31

McGoldrick, L. F. 1970a. On Wilton's ripples: a special case of resonant interactions. *J. Fluid Mech.* 42: 193–200

McGoldrick, L. F. 1970b. An experiment on second-order capillary gravity resonant wave interactions. *J. Fluid Mech.* 40: 251–71

McGoldrick, L. F. 1972. On the rippling of small waves: a harmonic nonlinear nearly resonant interaction. *J. Fluid Mech.* 52: 725–51

McGoldrick, L. F., Phillips, O. M., Huang, N. E., Hodgson, T. H. 1966. Measurements of third-order resonant wave interactions. *J. Fluid Mech.* 25: 437–56

McLean, J. W. 1982a. Instabilities of finite-amplitude water waves. *J. Fluid Mech.* 114: 315–30

McLean, J. W. 1982b. Instabilities of finite-amplitude gravity waves on water of finite depth. *J. Fluid Mech.* 114: 331–41

Meiron, D. I., Saffman, P. G., Yuen, H. C. 1982. Calculation of steady three-dimensional deep-water waves. *J. Fluid Mech.* 124: 109–21

Melville, W. K. 1982. The instability and breaking of deep-water waves. *J. Fluid Mech.* 115: 165–85

Mclville, W. K. 1983. Wave modulation and breakdown. *J. Fluid Mech.* 128: 489–506

Miles, J. W. 1984a. Nonlinear Faraday resonance. *J. Fluid Mech.* 146: 285–302

Miles, J. W. 1984b. On damped resonant interactions. *J. Phys. Oceanogr.* 14: 1677–78

Murakami, Y. 1987. Damped four-wave resonant interaction with external forcing. *Wave Motion* 9: 393–400

Ocean Wave Spectra Proceedings of a Conference, 1963. Englewood Cliffs: Prentice-Hall

Papadimitrakis, Y. A. 1986. On the structure of artificially generated water wave trains. *J. Geophys. Res.* 91: 14,237–49

Peregrine, D. H. 1983. Water waves, nonlinear Schroedinger equations and their solutions. *J. Austr. Math. Soc. Ser. B* 25: 16–43

Perlin, M., Hammack, J. 1991. Experiments on ripple instabilities. Part 3. Resonant quartets of the Benjamin-Feir type. *J. Fluid Mech.* 229: 229–68

Perlin, M., Henderson, D., Hammack, J. 1990. Experiments on ripple instabilities. Part 2. Selective amplification of resonant triads. *J. Fluid Mech.* 219: 51–80

Phillips, O. M. 1960. On the dynamics of unsteady gravity waves of finite amplitude. Part 1. The elementary interactions. *J. Fluid Mech.* 9: 193–217

Phillips, O. M. 1967. Theoretical and experimental studies of gravity wave interactions. *Proc. R. Soc. London Ser. A* 299: 104–19

Phillips, O. M. 1974. Nonlinear dispersive waves. *Annu. Rev. Fluid Mech.* 6: 93–110
Phillips, O. M. 1977. *The Dynamics of the Upper Ocean.* Cambridge: Cambridge Univ. Press. 2nd ed.
Phillips, O. M. 1981a. Wave interactions—the evolution of an idea. *J. Fluid Mech.* 106: 215–27
Phillips, O. M. 1981b. The dispersion of short wavelets in the presence of a dominant long wave. *J. Fluid Mech.* 107: 465–85
Pierson, W. J., Fife, P. 1961. Some nonlinear properties of long-crested periodic waves with lengths near 2.44 centimeters. *J. Geophys. Res.* 66: 163–79
Plant, W. J., Wright, J. W. 1979. Spectral decomposition of short gravity wave systems. *J. Phys. Oceanogr.* 9: 621–24
Ramamonjiarisoa, A., Coantic, M. 1976. Loi experimental de dispersion des vagues produites par le vent sur une faible longueur d'action. *C. R. Acad. Sci. Paris Ser. B* 282: 111–13
Ramamonjiarisoa, A., Mollo-Christensen, E. 1979. Modulation characteristics of sea surface waves. *J. Geophys. Res.* 84: 7769–75
Ramamonjiarisoa, A., Mollo-Christensen, E. 1981. Reply. *J. Geophys. Res.* 86: 2076–77
Rayleigh, Lord 1890. On the tension of water surfaces, clean and contaminated, investigated by the method of ripples. *Phil. Mag.* 30: 386–400
Resio, D., Perrie, W. 1991. A numerical study of nonlinear energy fluxes due to wave-wave interactions. Part 1. Methodology and basic results. *J. Fluid Mech.* 223: 603–29
Scott, J. C. 1981. The propagation of capillary-gravity waves on a clean water surface. *J. Fluid Mech.* 108: 127–31
Segur, H. 1984. Toward a new kinetic theory for resonant triads. *Contemp. Math.* 28: 281–313
Sell, W., Hasselmann, K. 1972. Computations of nonlinear energy transfer for JONSWAP and empirical wind wave spectra. *Rep. Inst. Geophys.*, Univ. Hamburg
Simmons, W. F. 1969. A variational method for weak resonant wave interactions. *Proc. R. Soc. London Ser. A* 309: 551–75
Stiassnie, M. 1984. Note on the modified nonlinear Schroedinger equation for deep water waves. *Wave Motion* 6: 431–33
Stiassnie, M., Shemer, L. 1984. On modifications of the Zakharov equation for surface gravity waves. *J. Fluid Mech.* 143: 47–67
Stiassnie, M., Shemer, L. 1987. Energy computations for evolution of class I and II instabilities of Stokes waves. *J. Fluid Mech.* 174: 299–312
Stokes, G. G. 1847. On the theory of oscillatory waves. *Cambridge Philos. Soc. Trans.* 8: 441–55
Su, M. Y. 1982. Three-dimensional deep-water waves. Part 1. Experimental measurement of skew and symmetric wave patterns. *J. Fluid Mech.* 124: 73–108
Su, M. Y., Bergin, M., Marler, P., Myrick, R. 1982. Experiments on nonlinear instabilities and evolution of steep gravity-wave trains. *J. Fluid Mech.* 124: 45–72
Su, M. Y., Green, A. W. 1984. Coupled two- and three-dimensional instabilities of surface gravity waves. *Phys. Fluids* 27: 2595–97
Trulsen, K., Dysthe, K. B. 1990. Frequency down-shift through self modulation and breaking. In *Water Wave Kinematics.* 178: 561–72. Dordrecht: Kluwer (Applied Sci., Ser. E)
Valenzuela, G. R., Laing, M. B. 1972. Nonlinear energy transfer in gravity-capillary wave spectra, with applications. *J. Fluid Mech.* 54: 507–20
van Gastel, K. 1987a. Nonlinear interactions of gravity-capillary waves: Lagrangian theory and effects on the spectrum. *J. Fluid Mech.* 182: 499–523
van Gastel, K. 1987b. Imaging by *X* band radar of subsurface features: a nonlinear phenomenon. *J. Geophys. Res.* 92: 11,857–65
von Matthiessen, L. 1889. Experimentelle Untersuchungen ueber das Thomson'sche Gesetz der Wellenbewegung auf Fluessigkeitein unter der Wirkung der Schwere und Cohaesion. *Ann. Phys.* 38: 118–30
Watson, K. M., West, B. J. 1975. A transport-equation description of nonlinear ocean surface wave interactions. *J. Fluid Mech.* 70: 815–26
Webb, D. J. 1978. Non-linear transfers between sea waves. *Deep-Sea Res.* 25: 279–98
Weiland, J., Wilhelmsson, H. 1977. *Coherent Non-linear Interaction of Waves in Plasmas*, 88. New York: Pergamon. (Int. Ser. Natural Philos.)
West, B. J. 1981. *Deep Water Gravity Waves*, 146. New York: Springer-Verlag
Whitehead, A. N. 1958. *An Introduction to Mathematics.* New York: Oxford Univ. Press
Whitham, G. B. 1967. Non-linear dispersion of water waves. *J. Fluid Mech.* 27: 399–412
Whitham, G. B. 1974. *Linear and Nonlinear Waves.* New York: Wiley-Interscience
Wilhelmsson, H., Pavlenko, V. P. 1973. Five wave interaction—a possibility for enhancement of optical or microwave radiation by nonlinear coupling to explosively unstable plasma waves. *Phys. Scr.* 7: 213–16

Willebrand, J. 1975. Energy transport in a nonlinear and inhomogeneous random gravity wave field. *J. Fluid Mech.* 70: 113–26

Wilton, J. R. 1915. On ripples. *Phil. Mag.* 29: 688–700

Wu, H.-Y., Hsu, E.-Y., Street, R. L. 1979. Experimental study of nonlinear wave-wave interaction and white-cap dissipation of wind-generated waves. *Dyn. Atmos. Oceans* 3: 55–78

Yuen, H. C., Lake, B. M. 1975. Nonlinear deep water waves: theory and experiment. *Phys. Fluids* 18: 956–60

Yuen, H. C., Lake, B. M. 1980. Instabilities of waves on deep water. *Annu. Rev. Fluid Mech.* 12: 303–34

Yuen, H. C., Lake, B. M. 1982. Nonlinear dynamics of deep-water gravity waves. *Adv. Appl. Mech.* 22: 67–229

Zakharov, V. E. 1968. Stability of periodic waves of finite amplitude on the surface of a deep fluid. *J. Appl. Mech. Tech. Phys.* 2: 190–94. (From Russian)

Zakharov, V. E., Shabat, A. B. 1972. Exact theory of two-dimensional self-focusing and one-dimensional self-modulation of waves in nonlinear media. *Sov. Phys. JETP* 34: 62–69

Zhang, J., Melville, W. K. 1987. Three-dimensional instabilities of nonlinear gravity-capillary waves. *J. Fluid Mech.* 174: 187–208